UNIVERSITY OF TWENTE.

Faculty of Engineering Technology

Identifying impact damage with the use of Piezoelectric transducers in a phased array

Xander C. van Hal

B.Sc. Thesis

June 2021

Supervisors:
dr. ir. R. Loendersloot
dr. D. Di Maio

Dynamics Based Maintenance
MS3
University of Twente
P.O. Box 217
7500 AE Enschede
The Netherlands

Abstract

In this report, the niche field of damage identification using phased array theory is explored. Piezoelectric transducers can send and receive wave signals. Upon using time delay between the several wave signals sent, a focused phased array can be established. The phased array is based on constructive interference and will create a signal of larger amplitude, which can be directed. To establish the successfulness of the focusing of the phased array, several experiments were conducted as presented in this study. Iterating over the time delay was found to be the best method to implement the phased array theory in damage identification.

Contents

1 Introduction

Composite materials are a combination of two materials. They have better material properties in tandem compared to on their own [1]. Composite materials are created to optimalize their properties, ranging from the yield stress number to weight. Various fields can benefit from these enhanced material properties, among which is the aerospace industry. For instance, the Boeing 787, a fairly recently developed aircraft, consists out of these composite materials for 50% [2]. This decreases the total weight of the plane which is beneficial for e.g. fuel consumption.

Despite its improved properties, damage can still occur in composites. It can be complicated to detect this damage in time. Therefore, various methods have been developed for this purpose in past years. Examples of these are ultrasonic testing, X-rays and vibration, or model analysis [3]. One of these methods is the topic of this research paper, a damage detection mechanism based on ultrasonic testing with Piezoelectric transducers.

When impact damage occurs in a composite, it should be detected and located, which can be achieved through an ultrasound-based interrogation with Piezoelectric transducers [4]. One transducer is called the actuator, whilst the other transducers receive the signal sent by the actuator. This set-up is also known as the pitch-catch configuration [5]. If the signal differs from the default signal, it is likely that some kind of deviation has occurred on the path the signal has travelled, possibly caused by impact damage. Upon using multiple of these Piezoelectric transducers, the entire composite can be analysed with this method in addition to the location and the severity of the impact damage.

Multiple Piezoelectric transducers can also be used to form a phased array [6]. A wave signal with a bigger amplitude can be generated at the point of damage and thus more information can be extracted from this signal once it arrives at a receiver. This is done through sending the signals with a small time delay sequentially. This will cause constructive and destructive interference of the different wave signals sent in a certain direction. The waves amplify each other and thus a signal with a bigger amplitude is created.

Nevertheless, it is not yet fully known how much more additional information can be obtained from the wave signal using this phased array. Additionally, it is difficult to locate where the constructive interference of the phased array occurs.

The purpose of this bachelor thesis is to better understand this niche of damage identification, using phased arrays to extract more information on impact damage. This will be done by collecting data using experiments and analyzing said data. A more specific research question has to be set, which will be discussed in the following section.

2 Research question

The research question is divided into several sub-questions to address the full scope of the issue at hand. Afterwards, a discussion on the problem definition answered in the sub-questions will take place.

2.1 Problem

To retrieve more information about the impact damage details on a composite plate, a phased array measuring method can be used. Multiple Piezoelectric transducers send a signal with a time delay and thus a phase delay. The delay allows the different signals to interfere with each other; at certain angles they combine and amplify one another, whilst in other directions they will dampen.

Past research has shown that the interference of these signals does occur [7]. It is, however, still unknown how the direction of this interference can be steered as well as its precision. Consequently, it is currently unknown how the phased array signal will vary when travelling through impact damage, since the steering and precision of direction of focus is unknown.

It should be taken into account that the plate is considered quasi-isotropic. Since it is not fully isotropic, the shaping of the phased array can be influenced by material properties. This may cause the phased array focus in unexpected directions. Moreover, previous research showed that the resolution of the signal can be enhanced to retrieve better measurement data [7]. The careful selection of frequencies is also important, since these influence the measurement data.

2.2 Research question

How can signals with a better resolution enhance the observation of damage in a composite plate using a phased array measuring method?
Several aspects come into play when answering this research question, such as the optimal frequencies for the experiments in addition to the placement of the area where the interference of the Piezoelectric transducers occurs. Furthermore, the focusing into the correct direction should be noted. This will increase the amplitude and, therefore, influence the resolution of the signal.

2.3 Sub-questions

To answer the main research question, several sub-questions have been set. They will be discussed below.

1. **In what way can the resolution of the signal arriving at the receivers be enhanced?**
   In this sub-question, the resolution of the received signals of the guided lamb waves will be investigated to determine how they can be enhanced during these experiments.

2. **What frequencies will be used during the experiments?**
   At certain frequencies, the guided lamb waves can travel for a longer distance through the composite. Whilst doing so, they pick up more information about the damage. These frequencies can be detected using dispersion curves. It should also be investigated how effectively the signals with these frequencies are transmitted into the material, such that useful frequencies can be found to analyze the impact damage with.

3. **How can the focused area of the phased array be changed?**
   To obtain a better image with a higher resolution of the damage, the focused area of the phased array should be located onto this damage. It is, therefore, necessary to analyze how the focused area can be changed by adapting the parameters of the different Piezoelectric transducers.

4. **What does the signal look like when passing damage in comparison to not passing damage?**
   The differences between signals travelling through damage and signals not travelling through damage can be found once all the other sub-questions are answered. These results can be used to answer the overall research question. Several parameters such as the used frequencies have been addressed in the previous sub-questions.

2.4 Approach

First, a literature review will be conducted. This literature review will be used to gain a better understanding of the concept of damage identification. Furthermore, this literature review can be used to answer the questions regarding what frequencies will be used and what the theoretical concept behind the focusing is based on a phased array.

Once this is achieved, measurements can be performed to test the theoretical concept of focusing. This is done through focusing on a certain receiver and the signal arriving at this receiver that should be measured. Then, the signal should be analyzed to discover whether superposition of the signal has occurred in the direction of this receiver. If this theoretical concept of focusing does behave as expected, other ways should be researched to create a phased array in a certain direction. If done successfully, measurements can be performed on areas the signal is focused in the direction of the impact damage. Finally, the data found through these last experiments can be used to analyze how the signal differs upon passing through impact damage versus when not passing through this type of damage.

3 Theoretical background

In this section, the theoretical background on the identification of impact damage using Piezoelectric transducers will be discussed.

3.1 Composite materials

Composite materials are a combination of two materials that improve the overall material properties [1]. For example, stiffness can be increased to ensure that the composite material can be used for a greater variety of applications.

The composite material used for the experiments performed in this research is the so-called Carbon Fibre Reinforced Polymer (CFRP). This specific composite consists of fibre carbon and a polymer. It has multiple advantages, although it is accompanied by some disadvantages as well [8]. The most notable ones will be briefly elaborated on. Firstly, this combination of materials gives the composite a relatively higher specific and fatigue strength compared to its plastic counterpart. It is however lighter than materials such as steel and aluminium. Carbon fibre reinforced polymer can, therefore, be used for applications in the field of aerospace and aeronautics. The most notable downside is its price, which is high in comparison to alternatives such as steel.

The fibres of the Carbon Fibre Reinforced Polymer are added to the composite laminate to stiffen it. Their orientation with respect to the orientation of the composite laminate can differ [8]. A zero degree orientated placement of the fibres reacts to axial loads. A 45 degrees orientated placement reacts to shear loads and 90 degrees orientated placement reacts to side loads. The difference between these placements can be seen in figure 1.

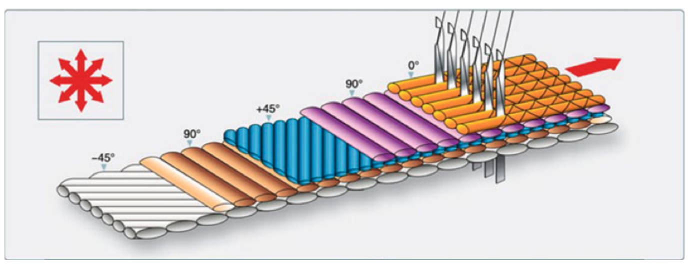

Figure 1: Different orientations of the fibres in layers with respect to the composite laminate [8].

If the fibres are placed in all the mentioned directions symmetrically and balanced, it is a quasi-isotropic composite. In this case the material has isotropic properties in-plane. Isotropic means that the composite has approximately the same strength and stiffness in the different directions of the composite [9]. How this quasi-isotropic case can be obtained in the case of the carbon fibre reinforced polymer, can be seen in figure 2.

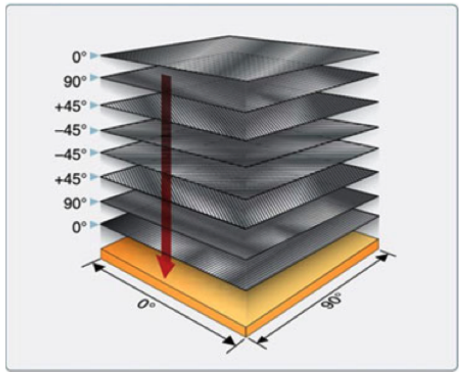

Figure 2: Placement of the fibres to obtain a quasi-isotropic composite [8].

The placement of the fibres has an influence on the propagation of the lamb waves through the material [10]. For the phased array method, it is assumed that the waves propagate omnidirectional. This implies that the waves propagate in all directions with the same velocity [11]. Practically, this is an assumption that cannot be fulfilled completely. This will have an influence on the outcome of the phased array method.

3.2 Guided lamb waves

There are several wave types which can be used for damage detection. The suitability of a wave type depends on the type of material, geometry and type and size of damage among others. For the application and material of the experiments conducted in this paper, guided lamb waves are most suitable [12]. These ultrasonic waves can propagate a long enough distance required for the experiments. Furthermore, they can be generated by the PWAS transducers discussed previously. Lamb waves generally consist of a superposition of longitudinal and shear modes [4]. The main difference between these two modes is orientation. The particles of longitudinal modes move parallel to the direction of wave propagation while the particles of shear modes are more perpendicular [13]. A visual representation of this can be seen in figure 3.

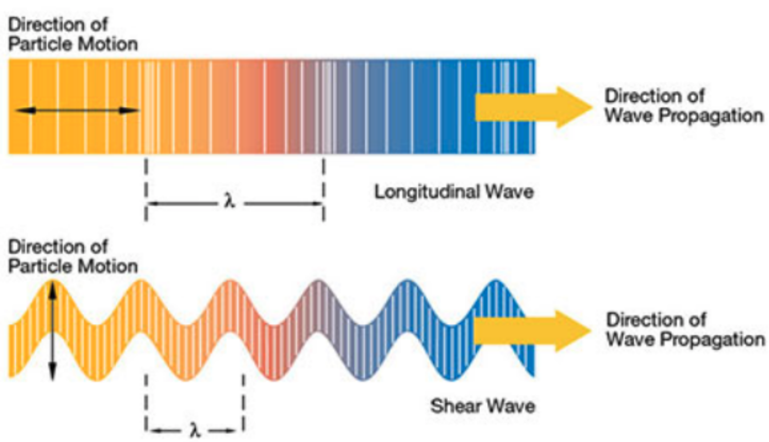

Figure 3: Difference between the motion of particles in longitudinal and shear waves [13].

Lamb waves can be either symmetric or anti-symmetric [4]. In case of symmetric waves, the modes of a lamb wave behave the same. For the anti-symmetric case, the modes of a lamb wave act exactly in the opposite direction. This can also be seen in figure 4. The symmetric wave is typically denoted as S_0 for the first mode. The first mode for the anti-symmetric wave is called A_0 [14]. The main difference between these cases is that S_0 wave modes travel at at a higher velocity than the A_0 ones [15]. Knowing this, the wave modes can be distinguished once they arrive at a receiver.

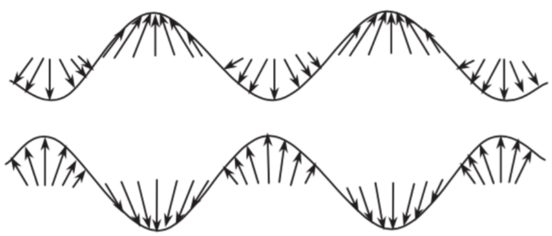

(a) Symmetric lamb mode.

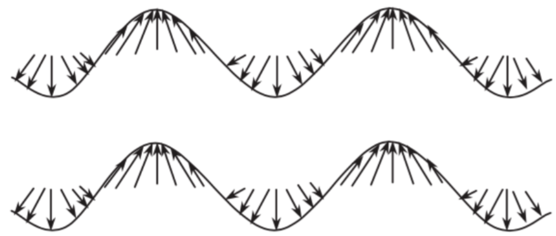

(b) Anti-symmetric lamb mode.

Figure 4: Types of lamb modes [4].

Guided lamb waves are a specific type of lamb waves. They are guided by two finite boundaries to ensure that they will propagate in one direction. These finite boundaries are the top and bottom of the material the waves propagate through. Consequently, they will arrive at the the receiver, allowing measurement of an output [4].

As discussed above, the guided lamb waves are generated using Piezoelectric transducers. This is the most suitable solution when applied to detect damage, since the input to the Piezoelectric transducers can be adapted in such a way that the desired guided lamb waves with the right characteristics can be obtained [4]. Nevertheless, it should be noted that guided waves are a complex type of waves due to the presence of dispersion for example [16]. As a result, the amplitude of the signal arriving at a receiver is lower, making it harder to read the signal.

3.3 Piezoelectric transducers

Piezoelectricity is the concept in which an electric charge is generated through squeezing or stretching of a Piezoelectric material. Piezoelectricity can be used in two ways [17]. The first one is direct Piezoelectricity, in which either squeezing or stretching of the Piezoelectric material causes a voltage to run, which can be measured. Secondly, converse Piezoelectricity exists, in which a voltage set on the Piezoelectric material causes this material to either squeeze or stretch. These different applications of Piezoelectricity can be seen in figure 5.

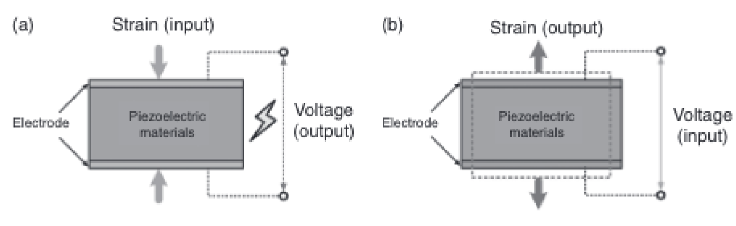

Figure 5: Effects of different applications of Piezoelectricity [17].

Piezoelectric Waver Active Sensors (PWAS) use Piezoelectricity to transmit and receive lamb waves through a structure. The stretch of the PWAS transducers cause the material they are attached to to vibrate, such that a wave can be sent through the material [18]. In this way, damage can be observed by measuring the wave signal received at certain points and comparing them to the transmitted signal. A visual representation of this can be seen in figure 6.

Figure 6: Visual representation of a lamb wave propagating through a structure [18].

There are two types of configuration that can be used with these piezoelectric transducers: pitch-catch and pulse-echo configuration [5]. In this case, the pitch-catch configuration is used. This means that the sending and receiving transducer are different transducers.

PWAS transducers have several advantages over other transducers when using propagation of waves to measure damage [18]. Firstly, PWAS transducers are attached to the structure using an adhesive bonding, which ensures greater adhesiveness to the surface compared to other more conventional transducers. Therefore, they transmit the waves through the structure more effectively. Secondly, they are non-resonant devices and, therefore, almost all frequencies can be used for PWAS transducers. Finally, they are relatively small and cheap in comparison to conventional transducers. Thus, they are available for a wider variety of applications. These are the reasons why they are convenient to use when detecting impact damage.

3.3.1 Received signal

The voltage of the arriving signal at the receiver is lower compared to the originally transmitted signal due to attenuation. The signal differs if the signal has come across impact damage on its path. This is distinguishable from a path without impact damage [6]. Therefore, it is necessary to take measurements of the signal when it has not encountered damage to establish the initial condition.

It should be noted that the A_0 mode of the wave has significantly more attenuation than the S_0 mode [19]. Since these modes also vary in travelling velocity, they arrive at separate moments at the receiving wave. The arriving S_0 mode has a higher amplitude in comparison to the A_0 mode, since it has less attenuation.

3.3.2 Single and phased array

The identification of the impact damage can be done by either using a single or a phased array [6]. In the case of the single array, a signal is sent by one Piezoelectric transducer, the actuator. After the signal has been sent, the different Piezoelectric transducers act as receiver and wait until they receive a signal. The difference found on this path with the signal travelling through undamaged specimen is then multiplied with a probability function for damage present on this path. When this is done for all paths on e.g. a plate, all values obtained are combined. In this way, damage can be identified on the path the signal has travelled [4]. An example of how this is done can be seen in figure 7.

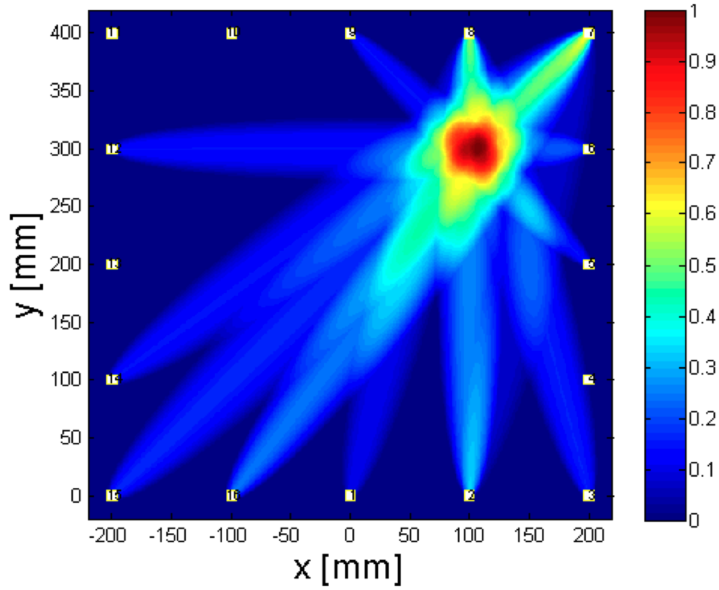

Figure 7: Identifying damage with the single array method. The red part shows the location of the damage [20].

Another option is to use multiple Piezoelectric transducers in a phased array. Here, multiple Piezoelectric transducers are used as actuators to send a signal with a short time intervals in comparison to each other and thus create a phase delay [21]. At certain places the wave signals damp each other out, whilst at other places they strengthen each other. The first and second case are respectively called destructive and constructive interference [22]. Locating this constructive interference in the direction of the damage, more information can be found about the damage once the signal arrives at a receiver. A visual representation of this can be seen in figure 8.

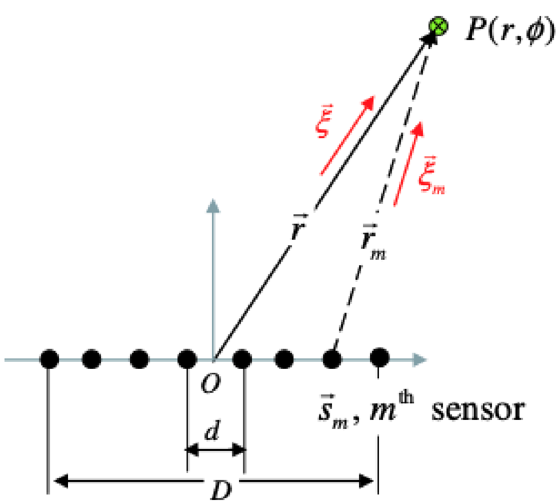

(a) Geometric representation of a phased array [21].

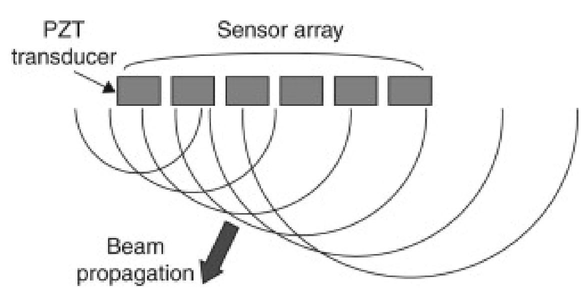

(b) Schematic representation of a phased array [17].

Figure 8: Different visual representations of a phased arrays.

The advantage of the phased array setup is the higher amplitude of the combined signal and therefore more information can be delivered to the receivers. As seen in figure 9, the location of inspection can be changed by adapting the angle θ of the transducers.

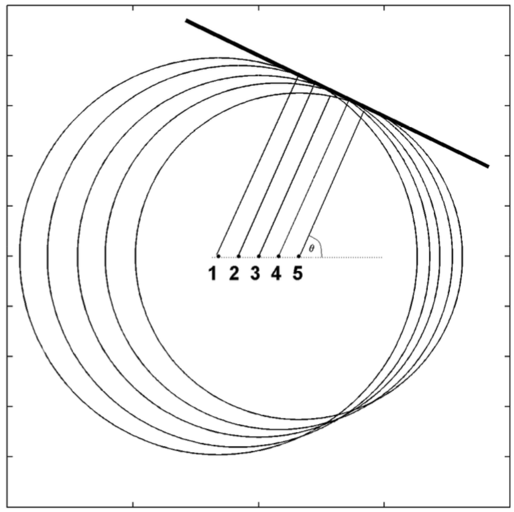

Figure 9: Constructive interference at a specific place with the use of a phased array [6].

$$t_i = \frac{l_i \cdot cos(\theta)}{c} \tag{1}$$

Equation (1) shows how this angle θ can be used to determine the time delay between the different Piezoelectric transducers. t_i is the time delay relative to the first transducer in seconds; l_i is the distance between the i-th and first transducer in m and c is the wave group velocity in m/s [6].

As discussed previously, combining the different wave signals and thus creating a signal with a higher amplitude is called constructive interference. This occurs when the wave signals are in phase. When the wave signals are out of phase, they cancel each other. This is called destructive interference [22]. Consequently, a relatively strong signal in one direction occurs as shown in figure 10.

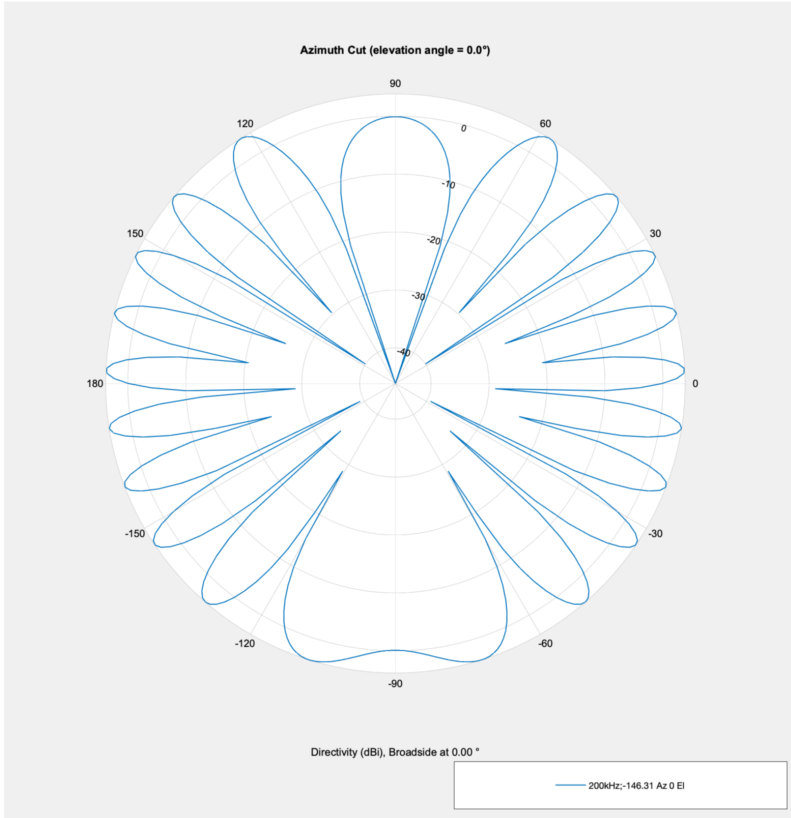

Figure 10: Matlab model of strength signal for phased array in different directions.

A clear difference between constructive and destructive interference can be observed in figure 10. The amount of side lobes present is interesting to note. This is in line with the theoretical background [21], when taking into account the parameters from the setup of the experiment. Due to the presence of these side lobes, the main lobe will be relatively smaller. Therefore, the amplitude of the combined phased array signal is smaller once arrived at the receiver. With awareness of the presence of these side lobes, analysis will run smoothly.

4 Experimental setup

This section discusses the setup of the conducted experiments. The equipment and software used will be described and reasoning given as to why certain parameters have been set to certain values.

4.1 Equipment

The setup consists of several pieces of equipment.
Firstly, the quasi-isotropic CFRP plate with three stiffeners through which the wave signal travels is used. A schematic representation of this plate can be seen in figure 11.

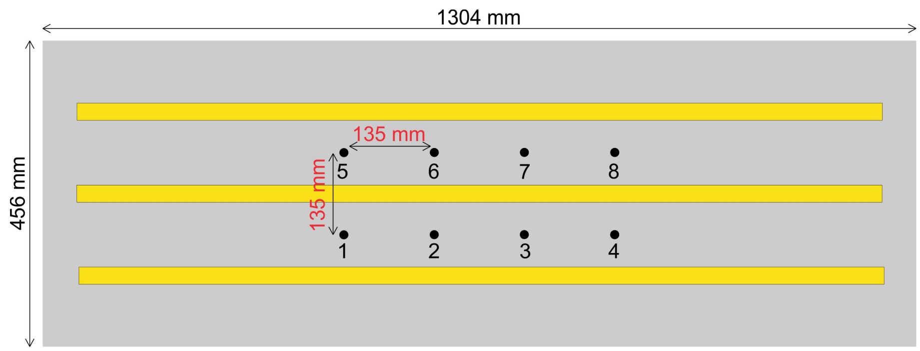

Figure 11: Schematic representation of the composite plate. The stiffeners are made yellow and the different dimensions can also be seen.

The thickness of the middle section of the plate is 2.1mm and consists of 16 layers of carbon fibre. The three T-shaped stiffeners run along the middle of the plate. Figure 12 shows that the damage is located near the middle of PWAS2, PWAS3, PWAS6 and PWAS7. This damage was created using an impact machine. The plate was placed on foam at the corners to ensure it was dampened from nearby vibrations not connected to the experiment.

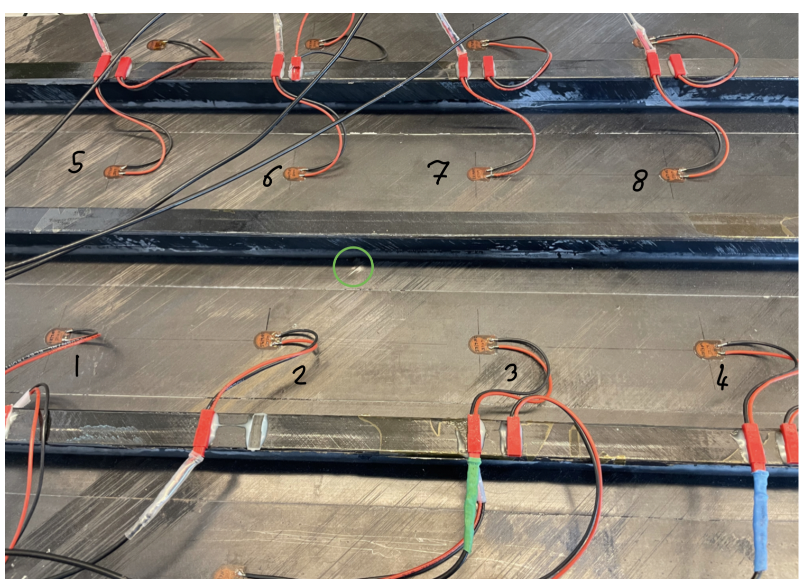

Figure 12: The composite plate, where PWAS1-4 are actuators and PWAS5-8 are receivers. The impact damage is indicated with the green circle.

A total of eight PWAS transducers is used; four as a transmitter, whilst the other four served as a receiver. A representation of this can be seen in figure 12. These PWAS transducers are circular PI DuraAct (PIC255) transducers, which have a thickness of 0.2mm and a diameter of 10mm.

The other part of the setup, which controls and measures the signals of the PWAS transducers, consists of several more parts. First, there is the NI PXI-e 1062Q chassis. This chassis synchronizes the timing of the modules.

To control this chassis and its modules via a computer, a remote controller is used. This is the NI PXIe-8301, which is connected to a laptop via Thunderbolt. Two NI PXI-6115 are connected to the chassis, which are used to take the measurements for both the input and the output. Finally, two NI TB-2708 modules are used to connect all these inputs and outputs to the amplifiers and finally to the PWAS transducers.

Four amplifiers were added to the setup, since previous research has shown that the amplitude of the A_0 mode is rather small when arriving at the receiver [7] and thus cannot be analyzed correctly due to noise. Furthermore, the setup was not always able to create a 10 V amplitude wave signal. This was especially the case for the wave signals with a frequency of 200 kHz and higher [7]. An amplifier will also help in solving these problems, since the amplitude of the wave signal easily reaches 10 V or more now. This helps when analyzing the results.

4.2 Controlling the setup

The setup is controlled using the program LabVIEW. Certain parameters are entered into the LabVIEW program. Afterwards, the LabVIEW program initializes the transducers and ensures that the correct signals are sent to the correct transducers. This LabVIEW program also displays the output of the receiving transducers and saves this.

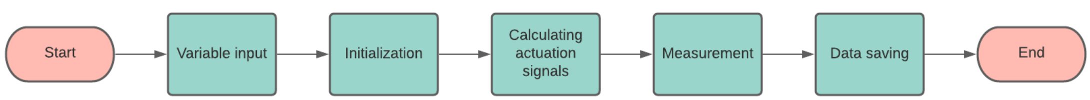

Figure 13: Flowchart of the measurements using the program LabVIEW.

The LabVIEW program consists of 5 phases. The flowchart can be seen in figure 13. Per phase, a short description is given in the section below.

1. **Variable input phase**
   It has to be decided on which receiving PWAS is focused. The frequency, amplitude and number of cycles of the actuation signal also need to be entered. Additionally, the measurement time and number of averages, which is the number of times the measurement is conducted, have to be filled out. Finally, the time of flights from the different sending PWAS to the focused receiving PWAS should be filled out. The time of flights can be used to find the average phase velocity of the wave signals.

   In this variable input phase, the time delay between the different actuating PWAS is calculated as well. For this, equation (1) is used. With a separate LabVIEW program, these time delays can be filled in manually or iterated over. These time delays are then calculated into bits and this information is sent to the next phase.

2. **Initialization phase**
The different sending and receiving channels of the NI chassis are initialized. The channels that read out the signal when actuated are set up. Then, the channels that read out when the signal is received are set up. Finally, the channels for the signal itself are set up. These last channels are then directed to the next phase. The other channels are directly sent to the measurement phase.

3. **Calculating actuation signals phase**
Using the variables that were entered and the calculated time delays, the different actuation signals for the phased array can be created. This is done by creating the actuation signal according to the different parameters. Afterwards, an array of zeros in bits is placed in front of this signal. The length of this array of zeros is determined by the time delay. All signals share the same length. This entire process has also graphically been shown in figure 14. When this is done, the signals are sent to the measurement phase.

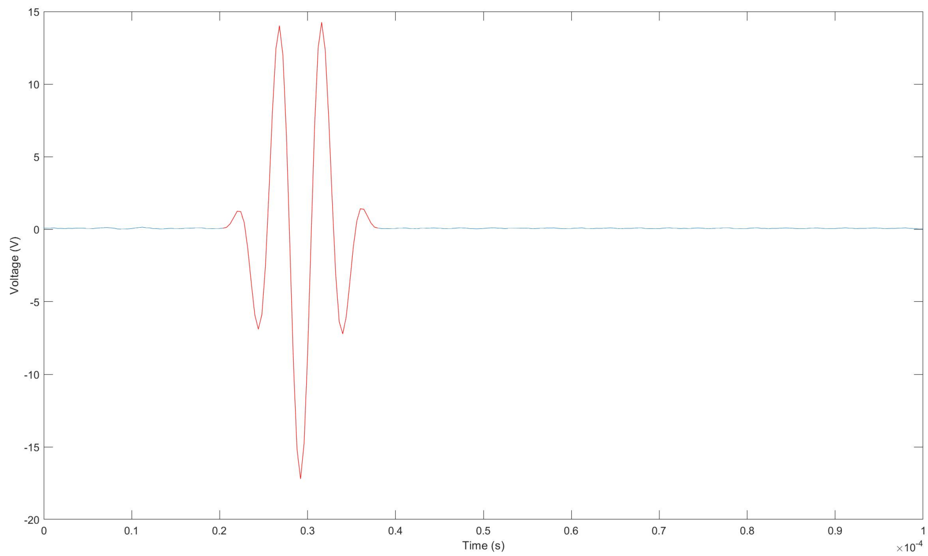

Figure 14: Graphical representation of signal with zeroes added. The blue and red part indicate respectively the zeros and signal.

4. **Measurement phase**
Having created the actuation signals, the different signals can be started at exactly the same moment. A trigger is used for this. The measurement phase ensures that, once the signals start to run, the different initialized reading channels are reading out. Once the measurement time has been reached, the reading is stopped. This phase is repeated for an entered number of averages to obtain more reliable results. Once this number of averages loop is finished, the signal is sent into the data saving phase.

5. **Data saving phase**
In the data saving phase, the different average signals for all the reading channels are saved into a TDMS file. Several other textual data are also saved to easily distinguish different measurements. This TDMS file is saved. Once completed, the program is finished and new measurements can be conducted.

4.3 Resolution of signal

To enhance the resolution of the signal received at the receivers, the focusing should be good enough such that it can focus on a certain receiver. This way, a higher amplitude signal will arrive at the receiver which can be used to get more information about the path the signal has travelled. In previous experiments, one actuator was not working and therefore only a phased array of three actuators was obtained [7]. In this research, the fourth actuator has been repaired and therefore a phased array of four actuators will be used. Apart from this, due to the maximum sampling rate of the National Instruments system I/O card, there were some problems with obtaining a signal which has a high enough amplitude. This problem occurred when doing measurements near 250 kHz [7]. This will be taken into account in the next section.

4.4 Used frequencies

It has been chosen to use 150 and 200 kHz as actuation frequency for the experiments conducted. There are several reasons to do so. First of all, a dispersion curve based on experimental results has been consulted. This dispersion curve can be seen in figure 15, where the yellow rectangle indicates the operational range of the research. It shows that the phase velocity for the A_0 and S_0 wave for a 150 kHz frequency is respectively 1400 and 5400 m/s. The phase velocities for the 200 kHz frequency are approximately the same. No other higher wave modes are present. The large differences in phase velocity for the A_0 and S_0 mode make these frequencies really usable, such that one measurements can be used for both modes. It is also nice to know that they travel at relatively high velocity through the composite.

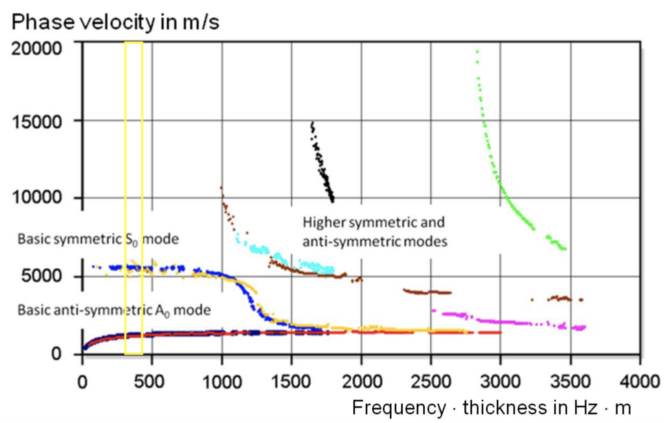

Figure 15: Dispersion curve of the phase velocity based on experimental results [23].

Secondly, a dispersion curve based on a theoretical model has been consulted. This dispersion curve can be seen in figure 16. The yellow rectangle is the area of interest for this research. The phase velocities are quite similar to the ones found in figure 15. It can however be seen that the A_1 wave is already present at a frequency of 200 kHz. To make sure that enough usable data will be collected, it has therefore been decided to also retrieve data at a frequency of 150 kHz. This will make the outcome of the experiment more reliable.

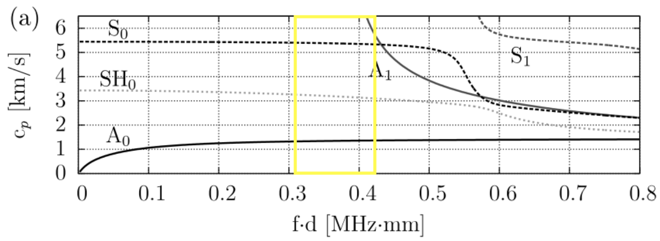

Figure 16: Dispersion curve of the phase velocity based on theoretical results [24].

Thirdly, it is important that the damage can be detected by different modes of the frequency. As written before, the A_0 mode travels at a velocity of 1400 m/s and the S_0 mode does so at a velocity of 5400 m/s. The damage should be at least half a wavelength λ to make sure that it is detected properly [12]. The wavelength can be determined with:

$$\lambda = \frac{v}{f} \tag{2}$$

Where λ is the wavelength in m, v is the velocity of the wave in m/s and f is the frequency in Hz.

The found wavelengths and required sizes of the damage for the different modes and frequencies can be seen in table 1. Since the damage is greater than these numbers, it can be detected at the frequencies discussed. It should however be noted that often even much smaller damages can be detected by the generated waves [12].

Table 1: Minimum damage size that can be detected for different wavelengths

	150 kHz, S_0	**150 kHz, A_0**	**200 kHz, S_0**	**200 kHz, A_0**
v (m/s)	5400	1400	5400	1400
λ (mm)	36.0	9.3	27.0	7.0
Minimum damage size (mm)	18.0	4.7	13.5	3.5

Therefore, based on the results found and that these frequencies were able to detect similar damage in previous experiments [7] the chosen frequencies 150 and 200 kHz can be used.

4.5 Focused area

The phased array signal starts in between the second and third actuator, as seen on figure 17. Several paths the phased array signal can travel when focused on a certain receiver can be seen in this figure as well, indicated by the green dashed lines.

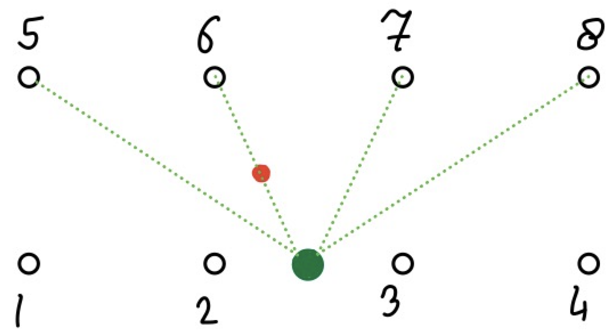

Figure 17: Schematic setup of the phased array experiment. The starting point and route of the phased array are respectively indicated with the green dot and green dashed lines. The location of the damage is shown in red.

To read out the signal at the receiver, the angle has to be changed such that the constructive interference occurs in the direction of the focused receiver. The angles that should be obtained can be seen in table 2.

Table 2: Angles that should be obtained for the phased array

	θ (°)
PWAS 5	146.31
PWAS 6	116.57
PWAS 7	63.43
PWAS 8	33.69

Since equation (1) is used to calculate the time delay between the sending transponders, it can be seen that the phased array of S_0 wave modes has different time delays in comparison to the one for the A_0 wave modes. Since phased arrays can be created with both of these modes, more experiments have to be conducted to fully analyze the capability of measuring impact damage with both the S_0 and A_0 wave modes. The measuring process for these different experiments will be discussed in the following section.

4.6 Measurement process

The measurement process consists of two sections. Firstly, the time of flight of both the S_0 and A_0 modes of the signal should be found, since these should be put into the LabVIEW program as discussed before. Secondly, the measurements for the phased array can be done. The measurements process for both of these sections will be described below.

4.6.1 Measurements for Time Of Flight (TOF)

To conduct these measurements, only one actuating transducer should be connected per measurement. The sent signal by this transducer can then be measured at the four different receiving transducers. These measurements should be repeated for the different sending transducers and actuation frequencies. Once this is done, signal analysis can be conducted such that the time of flights can be found. A more step-wise instruction can be found in section A.1.1.

The specific measurements that will be performed can be seen in the list below. The goal of each measurements is also given.

1. **TOF measurements**
   Frequency: 150kHz and 200 kHz
   Goal: Find TOF of signal travelling from different actuators to receivers.
   Actuating PWAS: PWAS1-2-3-4
   Receiving PWAS: PWAS5-6-7-8
   Analysis: Find TOF S_0 and A_0 signal.

4.6.2 Measurements for phased array

For these measurements, the time of flights should be filled in from the different sending transducers to the receiving transducer which is focused on. All these measurements should be repeated when focusing on the different receiving transducers and with the two different actuation frequencies. A more step-wise instruction can be found in section A.1.2. This instruction is focused on the first measurements in the list below. With small modifications, it can also be used for the other phased array measurements.

The different types of measurements that will be done for the phased array can be seen in the list below. Their goal is also given.

1. **Phased array (equation used, set to certain value)**
   Frequency: 150 kHz and 200 kHz
   Goal: Create a phased array based on formula (1) and perform measurements to check whether this works.
   Actuating PWAS: PWAS1-2-3-4
   Receiving PWAS: PWAS5-6-7-8
   Analysis: Check if superposition and focusing of signal occurs.

2. **Phased array (create with iterations of time delay)**
   Frequency: 200 kHz
   Goal: Iterate over the angles 0-180 degrees (and thus time delays) and find a peak. Afterwards, continue with one more actuator.
   Actuating PWAS: PWAS1-2, PWAS1-2-3, PWAS1-2-3-4
   Receiving PWAS: PWAS5-6-7-8
   Analysis: Find out whether this is best method to do focusing (by comparing both focusing of signal and time delay).

3. **Phased array (create with TOF found)**
   Frequency: 200 kHz
   Goal: Create a focused phased array based on the TOF found in previous experiments.
   Actuating PWAS: PWAS1-2-3-4
   Receiving PWAS: PWAS5-6-7-8
   Analysis: Find out whether this is best method to do focusing (by comparing both focusing of signal and time delay).

5 Results

In this section, the results and analysis will be presented.

5.1 Actuation signal

In figure 18, the actuation signals at a frequency of 150kHz can be seen for a phased array signal. The actuation signals at a frequency of 200kHz is shown in section A.2.1. It can be observed that the amplitude of actuating PWAS2 is smaller in comparison to the other actuating PWAS. This influences the results obtained from the phased arrays, since the smaller amplitude impacts the capability of the signal to create the superposition in a certain direction.

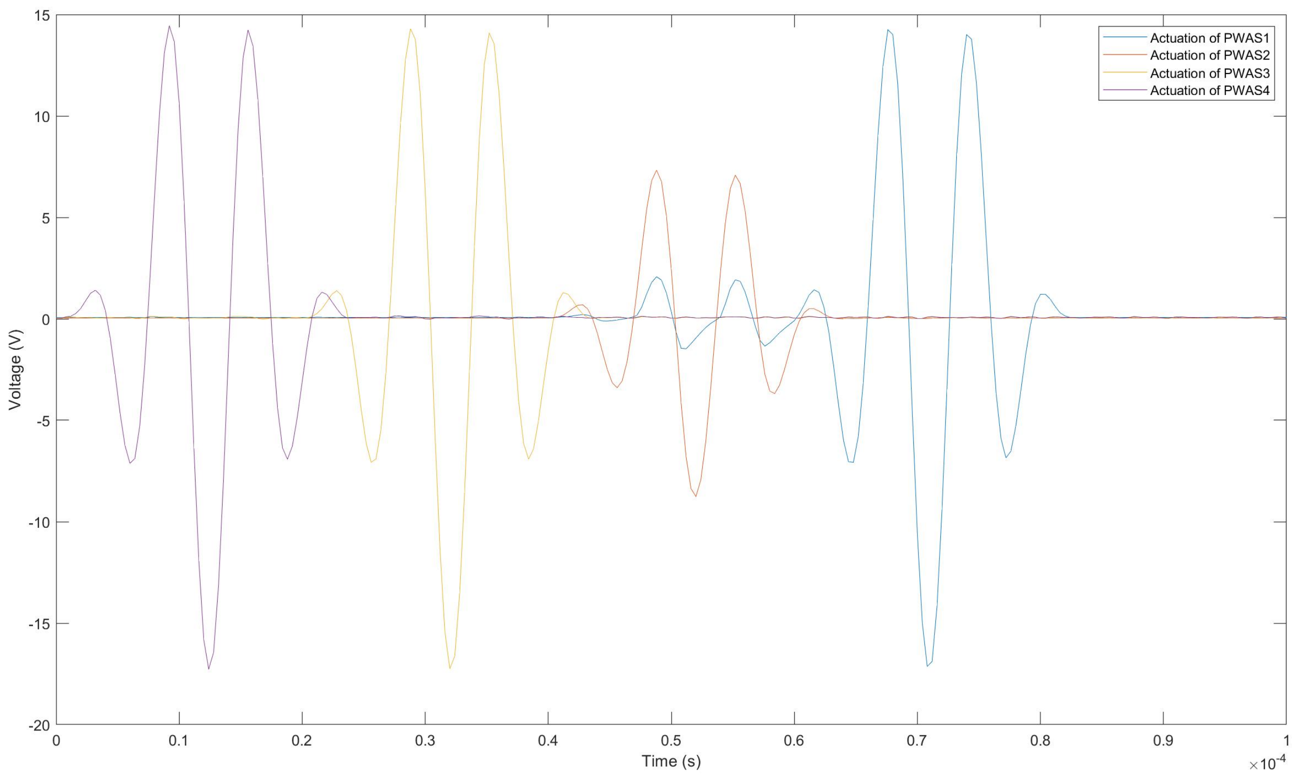

Figure 18: Actuation signals at a frequency of 150kHz.

5.2 Time of Flight

To compute the phased arrays, the time of flights of the different wave modes sent by the actuators have to be determined. Once these are known, the focus of the phased array can be set at a chosen receiver and measurements can be taken.

5.2.1 S_0 mode

An example of a single actuation signal sent by an actuator and how it arrives at the receiver can be seen in figure 19. The other single actuation signals is shown in section A.2.2.

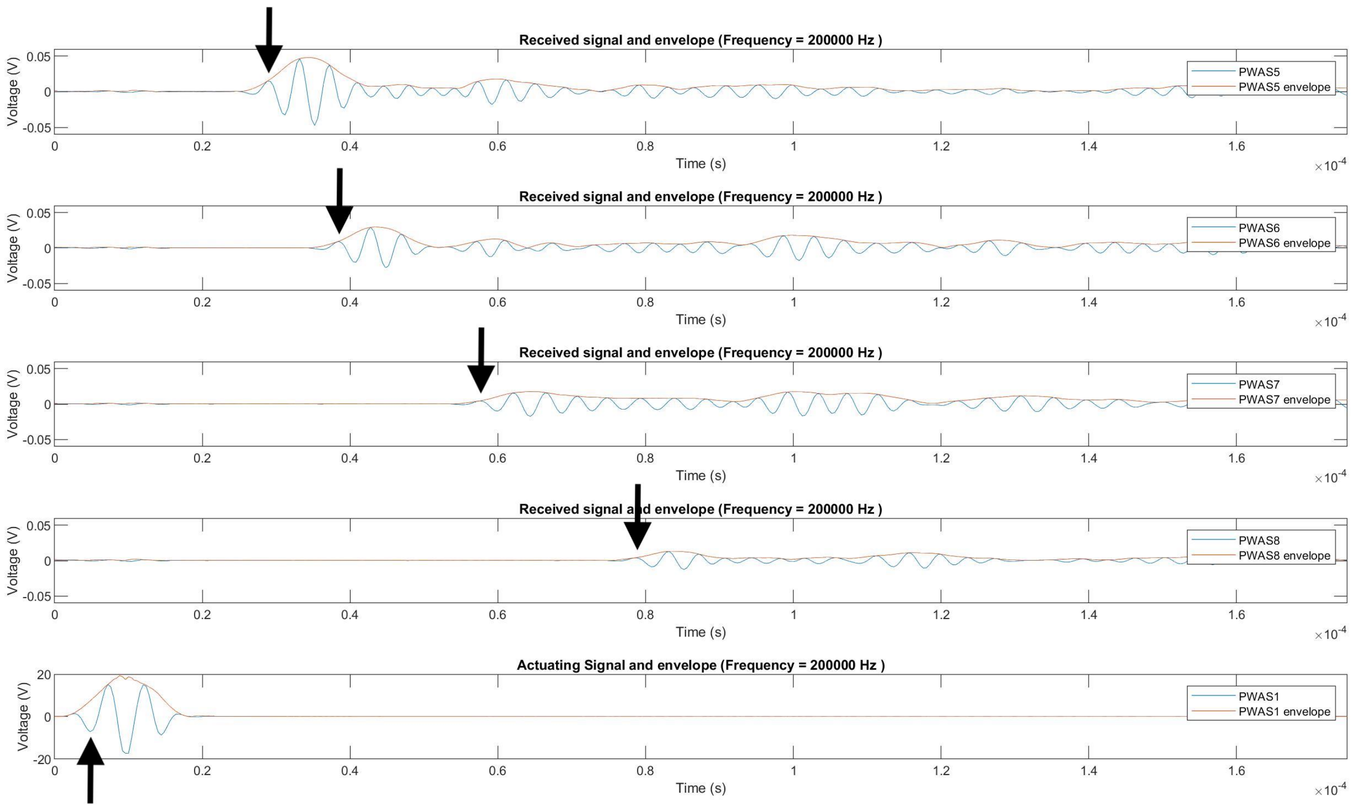

Figure 19: S_0 time of flight measurement with PWAS1 as actuator at 200kHz.

To determine the time of flight of the S_0 mode of the actuation signal, the time difference between one of the peaks at the actuation signal and this same peak at the received signal is taken. These peaks are indicated with arrows in figure 19. Because the S_0 mode travels at a higher velocity than the A_0 mode, it arrives at the receivers first. Consequently, the first signal arriving at the receivers is the S_0 mode which can be used to find the time of flight for the S_0 mode. This has been executed using Matlab, taking the absolute value of the signal. Hereafter, the peaks of the signal in question are determined. Once the received signal reaches the first peak with a minimum amplitude of circa 1e-3 V, the time of the peak is discovered and the time of this same peak at the actuation signal is subtracted. The minimum amplitude for the peak at the actuation signal was 0.2 V. These limits have been determined using experiments. Because the S_0 mode is the first to arrive, this method can quite accurately resemble the time of flights. Another method is finding the correlation between the sent and received signal.

The time of flights found can be seen in table 3 for 150kHz and table 4 for 200 kHz. Here the different columns represent the actuating PWAS and the different rows are the receiving PWAS.

Table 3: Time of flights for S_0 mode at 150kHz

150 kHz	**PWAS5**	**PWAS6**	**PWAS7**	**PWAS8**
PWAS1	2.36e-5 s	3.32e-5 s	5.24e-5 s	7.36e-5 s
PWAS2	3.32e-5 s	2.40e-5 s	3.68e-5 s	5.56e-5 s
PWAS3	5.24e-5 s	3.40e-5 s	2.48e-5 s	3.40e-5 s
PWAS4	7.36e-5 s	5.28e-5 s	3.48e-5 s	2.40e-5 s

Table 4: Time of flights for S_0 mode at 200kHz

200 kHz	**PWAS5**	**PWAS6**	**PWAS7**	**PWAS8**
PWAS1	2.40e-5 s	3.36e-5 s	5.52e-5 s	7.60e-5 s
PWAS2	3.36e-5 s	2.40e-5 s	3.60e-5 s	5.48e-5 s
PWAS3	5.28e-5 s	3.40e-5 s	2.48e-5 s	3.44e-5 s
PWAS4	7.36e-5 s	5.28e-5 s	3.44e-5 s	2.44e-5 s

Based on the found time of flights, the velocities can be calculated. These can be seen in table 5 for 150 kHz and table 6 for 200 kHz.

Table 5: Velocities for S_0 mode at 150kHz

150 kHz	**PWAS5**	**PWAS6**	**PWAS7**	**PWAS8**
PWAS1	5720 m/s	5750 m/s	5761 m/s	5800 m/s
PWAS2	5750 m/s	5625 m/s	5188 m/s	5430 m/s
PWAS3	5760 m/s	5615 m/s	5444 m/s	5615 m/s
PWAS4	5800 m/s	5718 m/s	5486 m/s	5625 m/s

Table 6: Velocities for S_0 mode at 200kHz

200 kHz	**PWAS5**	**PWAS6**	**PWAS7**	**PWAS8**
PWAS1	5630 m/s	5680 m/s	5470 m/s	5620 m/s
PWAS2	5680 m/s	5630 m/s	5300 m/s	5510 m/s
PWAS3	5720 m/s	5610 m/s	5440 m/s	5550 m/s
PWAS4	5800 m/s	5720 m/s	5550 m/s	5530 m/s

At 150kHz, the average velocity is 5630 m/s with a standard deviation of 169 m/s. At 200kHz, the average velocity is 5590 m/s with a standard deviation of 125 m/s. These velocities are slightly higher than the expected theoretical velocity of 5400 m/s, but considering that the standard deviation is relatively low these are really useful results to form a phased array.

5.2.2 A_0 mode

Since the A_0 mode of the actuation signal has more attenuation than the S_0 mode, determining the time of flight of this specific mode is complicated. The expected A_0 mode to arrive at the receiver looks indistinguishable from the actuation signal. It will, however, have a way lower amplitude than the S_0 mode due to its higher attenuation. As discussed in the theoretical background, the A_0 mode is more visible at lower frequencies. Therefore, the mode is expected to be most visually distinguishable at the lowest frequency measured, 150kHz.

To determine the time of flight of the A_0 mode, the estimated time the A_0 mode arrives at the receivers is highlighted by a blue line, as indicated in figure 20. The other figures of the analysis of the A_0 mode can be seen in section A.2.3.

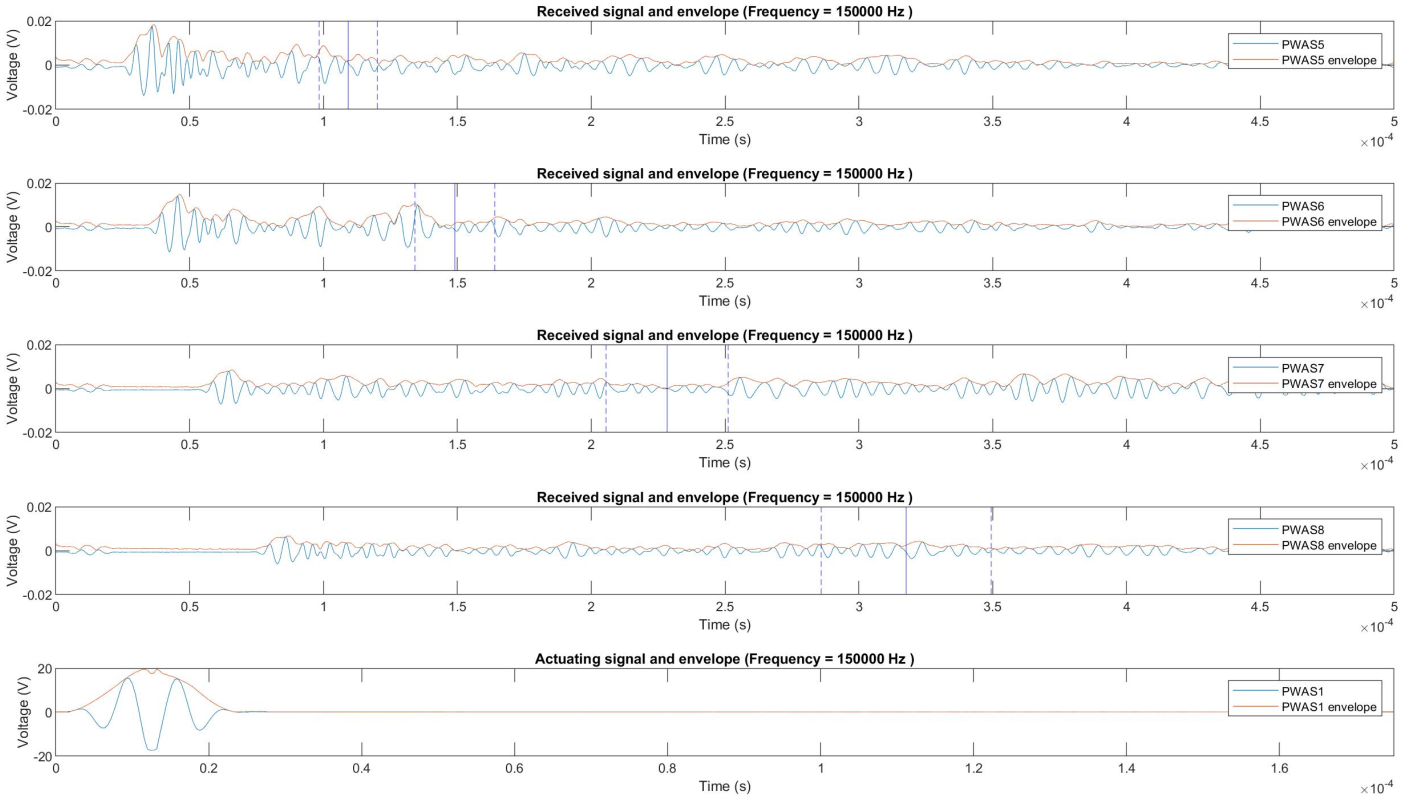

Figure 20: A_0 time of flight analysis, with PWAS1 as actuator at 150kHz.

This estimated time is based on the theory and a wave mode velocity of 1400 m/s. The dashed lines are the -10% and +10% error range of this estimated time. It is thus expected that the A_0 mode wave signal will arrive within this range. To discover the validity of this prediction, a pattern of the A_0 mode arriving should be noticed in this discussed range at the different receivers. For example, a wave shortly arriving before the blue line could be the A_0 mode. In that particular case, the wave would have travelled at a slightly higher velocity than the theory expected velocity. The other figures should then also show a A_0 mode signal, arriving shortly before the blue line.

This analysis has, however, shown that no time of flights for the A_0 mode can be found, due to too much attenuation. This was especially the case for the longer paths the signal had to travel, e.g. from PWAS1 to PWAS8. Because of this, no phased array based on the A_0 mode can be created.

5.3 Phased array (theoretical time delays)

Having established the time of flights of the S_0 mode, a phased array can be created. As discussed in the experimental setup, the occurrence of the superposition of the signal will first be checked. Afterwards, several methods will be used to establish how the focusing of the signal can be done.

5.3.1 Superposition of signal

To find out whether superposition of the signal happens, the single actuation signal of the closest actuating PWAS is compared to the focused phased array on a receiving PWAS. The two most notable data graphs found using this method can be seen in figures 21 and 22. The other graphs are presented in section A.2.4.

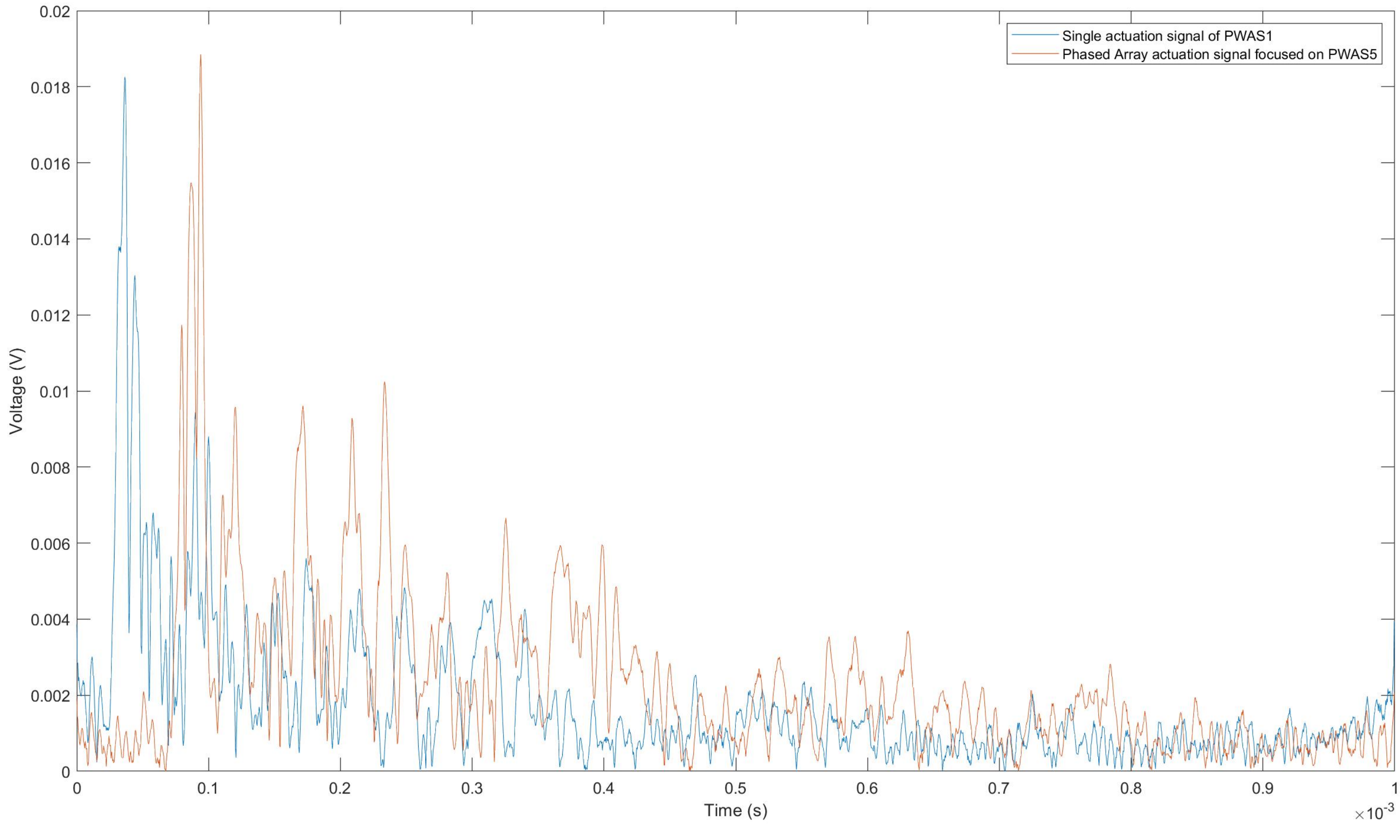

Figure 21: Single actuation of PWAS1 in comparison to phased array focused on PWAS5 at 150kHz.

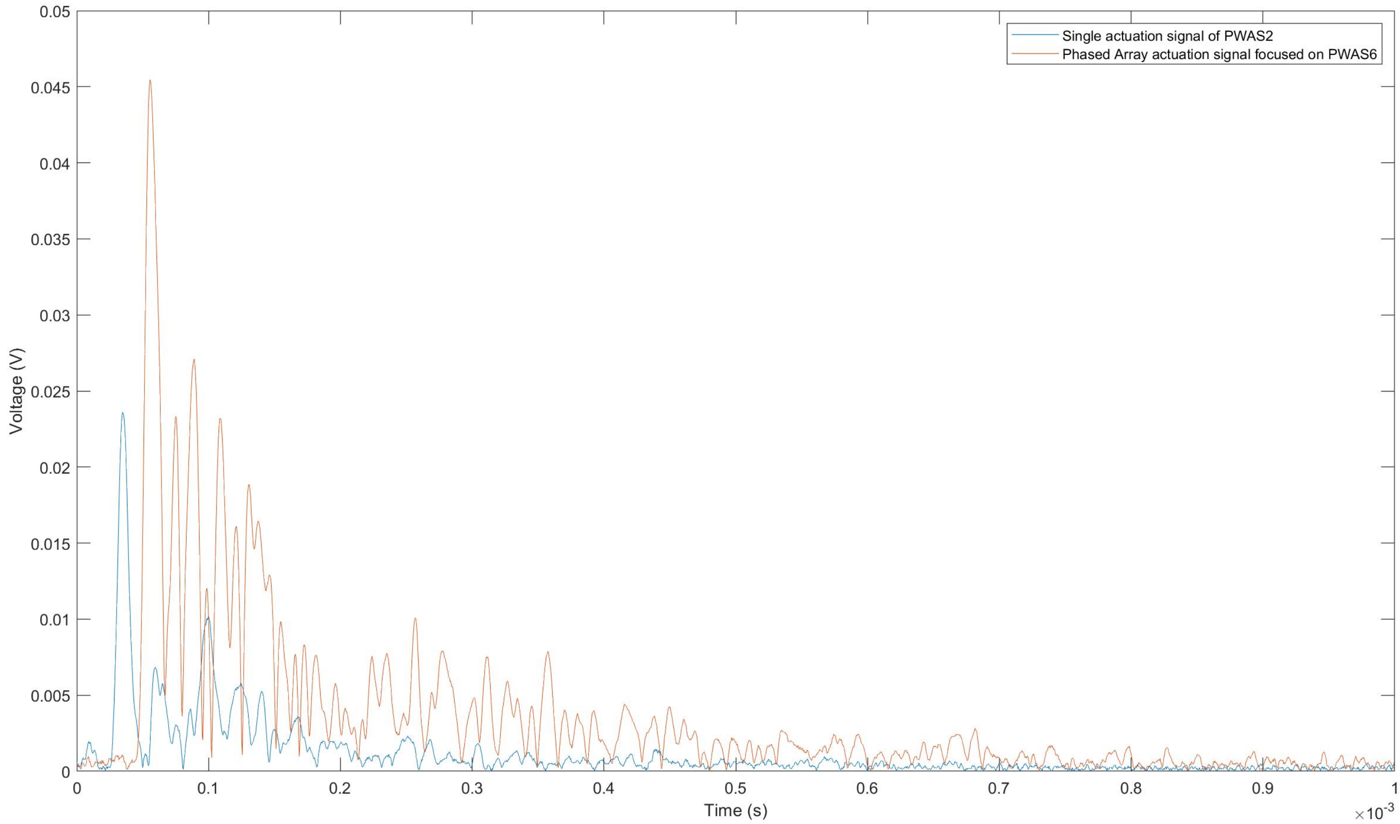

Figure 22: Single actuation of PWAS2 in comparison to phased array focused on PWAS6 at 200kHz.

To perform this analysis, the amplitude of the wave signal arriving at receiving PWAS is compared. If the maximum amplitude of the phased array signal surpasses the maximum amplitude of a single actuation, it can be concluded that superposition has occurred. Besides, the occurrence of the time of the phased array amplitude peak at different time intervals should be investigated as opposed to the occurrence at a single actuation. This is expected, since the superposition of the phased array arrives at a later time time than the single actuation signal.

Returning to figures 21 and 22, the amplitude of the largest peak of both signals in figure 21 appear largely similar. Nevertheless, knowing that they arrive at different time intervals at the receiver, it can be concluded that superposition occurs.

For figure 22, the amplitude of the largest peak of the phased array signal is circa twice as large as the peak of the single actuation signal. This is related to a smaller actuation signal; the superposition still occurs. At a later time moment, the peak of the phased array signal arrives at the receiver.

These measurements have also shown that a frequency of 200kHz is favourable over the frequency of 150kHz, as expected from the theory. The phased arrays created at 200kHz show a more focused beam compared to the phased arrays at 150kHz, which is also visible in the figures 21 and 22. Because of this, the 200kHz frequency will be used for further phased array measurements.

5.3.2 Focusing of signal

To discover whether the focusing of the signal occurs in the direction wanted, the signal arriving at a focused on receiver can be compared to the signal arriving at this receiver if not focused on. An example of this can be seen in figure 23.

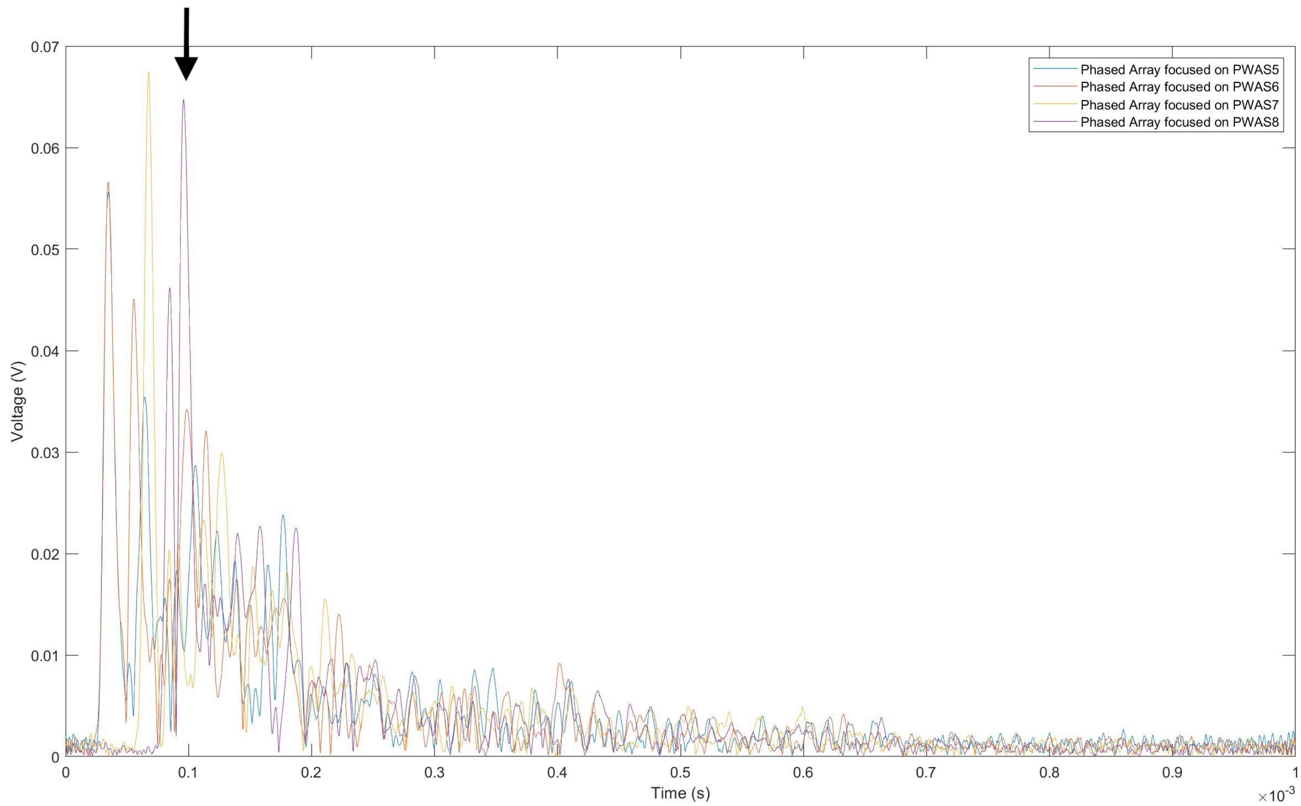

Figure 23: Signal received at PWAS8 when focusing on different PWAS. The arrow indicates the peak of the signal of the PWAS which is expected to be largest.

Since the signal is not largest when focused on this specific receiver, it can be concluded that the signal is not focused properly. This was the case for the majority of the measurements, as can be observed in section A.2.5.

5.3.3 Comparison of theoretical and experimental time delays

The expected time delays from the theoretical background will be compared to the experimentally discovered time delays to discover why the focusing of the signal did not occur in the right direction. These time delays determine how soon the signals of the different actuators are sent after each other. Using equation (1), the theoretical time delays can be found. These are given in table 7.

Table 7: Theoretical time delays when being focused on the different receivers

150/200 kHz	**To PWAS5**	**To PWAS6**	**To PWAS7**	**To PWAS8**
T0	0 s	0 s	0 s	0 s
T1	-2.08e-5 s	-1.12e-5 s	1.12e-5 s	2.08e-5 s
T2	-4.16e-5 s	-2.24e-5 s	2.24e-5 s	4.16e-5 s
T3	-6.24e-5 s	-3.36e-5 s	3.36e-5 s	6.24e-5 s

The experimental time delays can be found by determining how much longer it takes a signal to arrive at a certain receiver in comparison to the signal sent by the first actuator. For example, T1 is the time of flight from PWAS2 to PWAS5 minus the time of flight from PWAS1 to PWAS5. It is thus the time the signal actuated at PWAS2 has to travel extra in comparison to the first actuator, PWAS1. The values found with this method can be seen in table 8.

Table 8: Practical time delays found based on TOF when being focused on the different receivers

150/200 kHz	**To PWAS5**	**To PWAS6**	**To PWAS7**	**To PWAS8**
T0	0 s	0 s	0 s	0 s
T1	-9.60e-6 s	9.40e-6 s	1.74e-5 s	1.96e-5 s
T2	-2.88e-5 s	-6.00e-7 s	2.90e-5 s	4.06e-5 s
T3	-4.98e-5 s	-1.94e-5 s	1.92e-5 s	5.06e-5 s

For convenience, the results of 150 and 200 kHz were combined in one table. The average was taken of these.

When comparing the time delays found in tables 7 and 8, varying values can be observed. Firstly, the values found in table 7 are scaled linearly, whilst the values found in table 8 are not. This can be explained by the fact that the paths are not scaled linearly either. For example, the path between PWAS2 and PWAS5 is not twice the length as the path between PWAS1 and PWAS5; it is less. Therefore, it can be concluded that equation (1) is not suitable to use for this specific application.

However, taking into account the lengths of the different paths, table 8 still does not show expected time delays. An increase in time delay scales with the increase in length of the path was expected, since the material was assumed to be quasi-isotropic, resulting in omnidirectional waves. Because of this, it is useful to gain a better understanding on how the waves travel to the composite plate. About this, the section below will be.

5.4 Phased array (experimental time delays)

In this section, experiments conducted with experimental time delays will be discussed. Prior, a more detailed analysis on the composite plate will be given.

5.4.1 Composite plate analysis

Using the outcome of previous experiments, it has been shown that waves travelling perpendicular to the stiffeners travel at higher velocities than the waves travelling parallel to these stiffeners [25]. This causes the material properties of the composite plate vary in directions. Therefore, equation (1) cannot be used in this research. The next best option is creating individual time delays for each actuating PWAS. This can be done through types of experiments, about which more can be read in the following section.

5.4.2 Iterating over time delay

To obtain a better focused phased array beam at a receiver, varying angles are iterated over (based on equation (1)) and thus different time delays. The signals arriving at PWAS6 for different time delays can be seen in 24. The other plots are shown in section A.2.6.

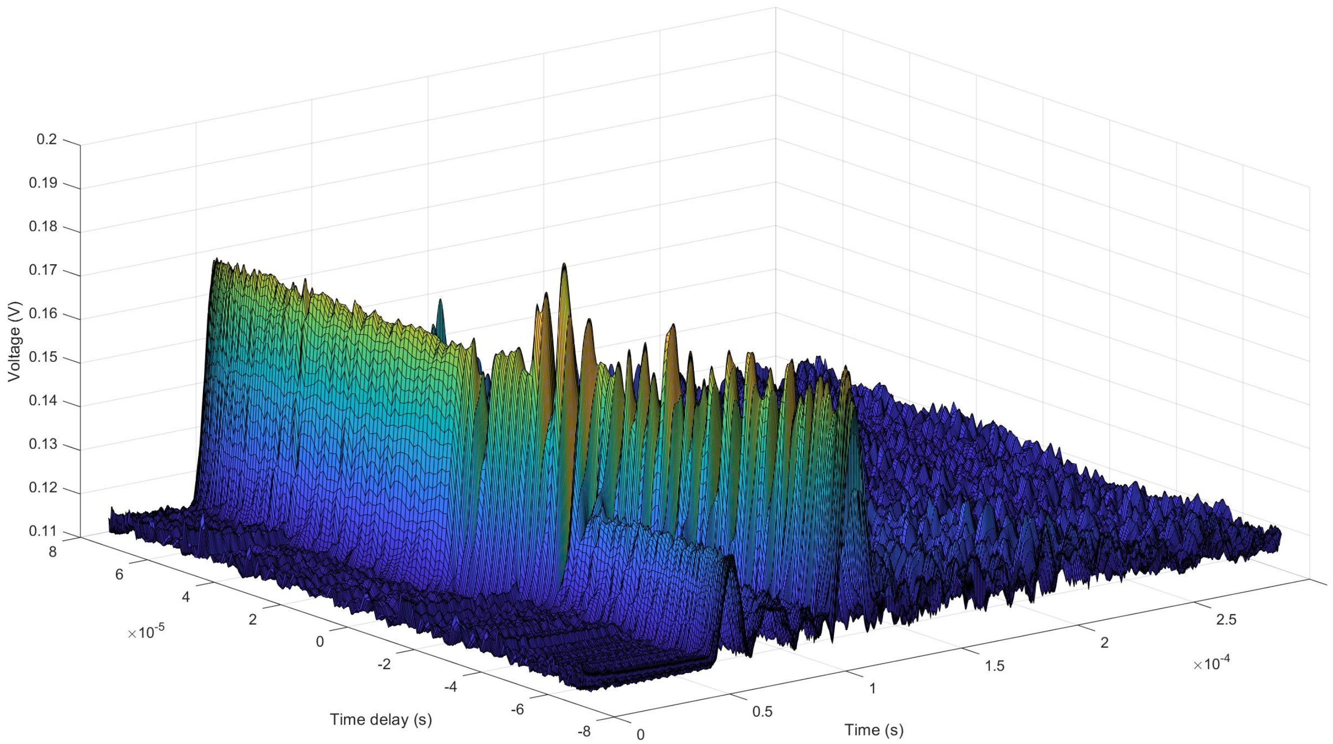

Figure 24: Signal received at PWAS6 for phased array focused on PWAS6, iterating over the time delay between PWAS1 and PWAS4. Other time delays are set to certain value based on previous measurements.

These results have been created by starting with a phased array of actuator PWAS1 and PWAS2 which is then iterated over the angles 0 to 180 degrees. These angles are entered into equation (1) and the results of this are shown in figure 25. The maximum signal strength is plotted here for all time delays. This clarifies the analysis enabling the creation of a phased array in the desired direction.

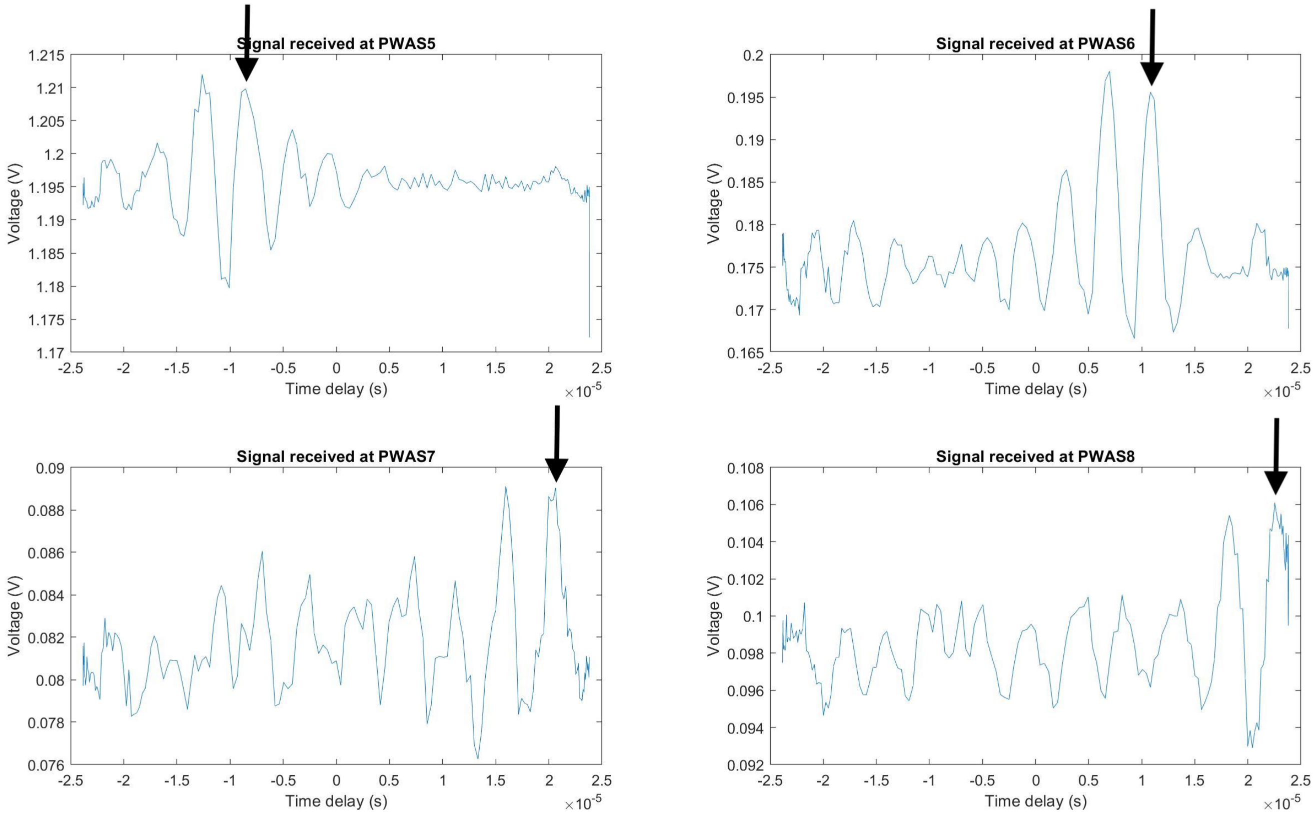

Figure 25: Signal arriving at receivers for different time delays. PWAS1 and PWAS2 are actuating. The peaks which are used for building the phased arrays are indicated with the arrows.

The arriving signal at a receiver, e.g. PWAS6, has several peaks for different angles. Based on the angle and equation (1), the time delay between PWAS1 and PWAS2 can be found and made constant. Next, the third actuator has been added to create a phased array of the actuators PWAS1, PWAS2 and PWAS3. Time delays will be iterated over once more to find a new peak. The results of this can be seen in figure 26.

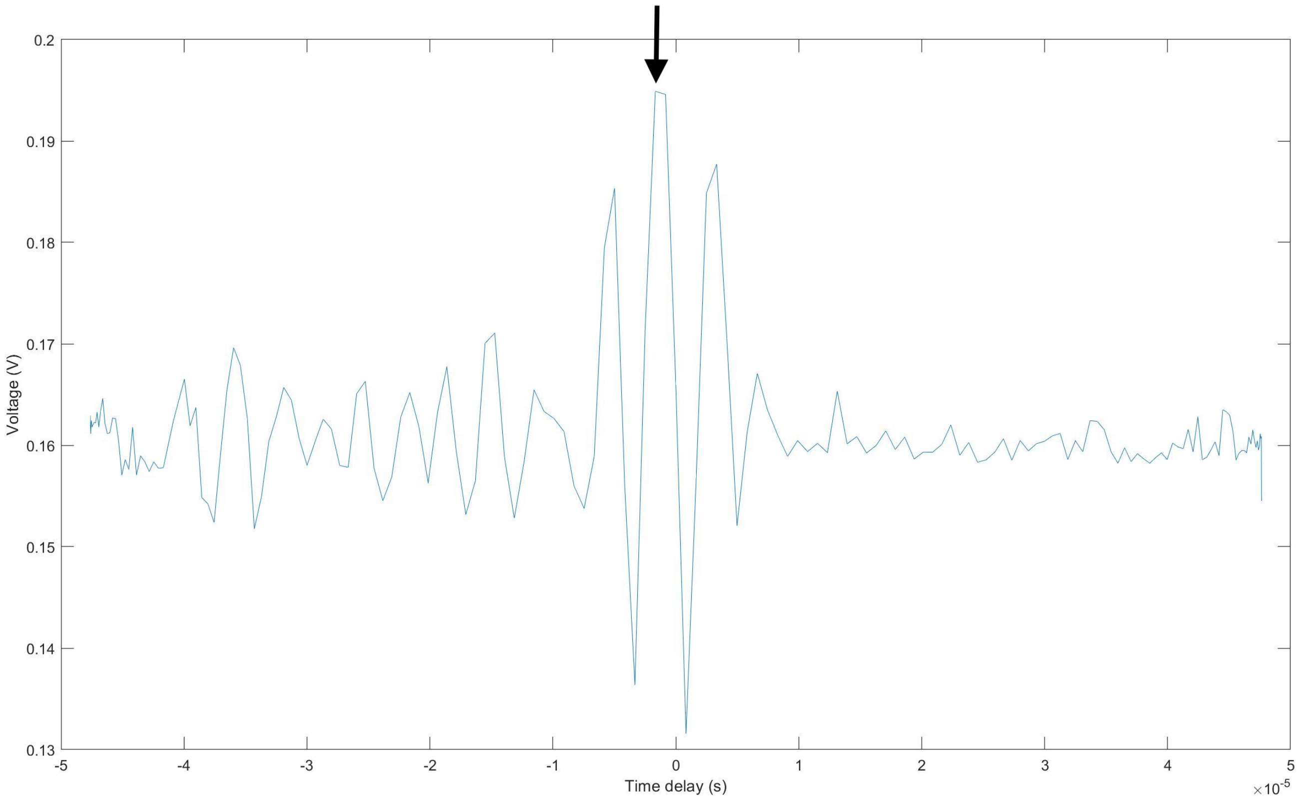

Figure 26: Focus on PWAS6. Signal arriving at receiver PWAS6 for different time delays. Time delay between PWAS1 and PWAS2 is constant, between PWAS1 and PWAS3 is variable. The arrow indicates the time delay where the phased array arrives at the receiver.

Finally, the same procedure can be repeated by adding the fourth actuator and thus having a phased array of all actuators. The result of this can be seen in figure 27. All other figures of this method can be seen in section A.2.7.

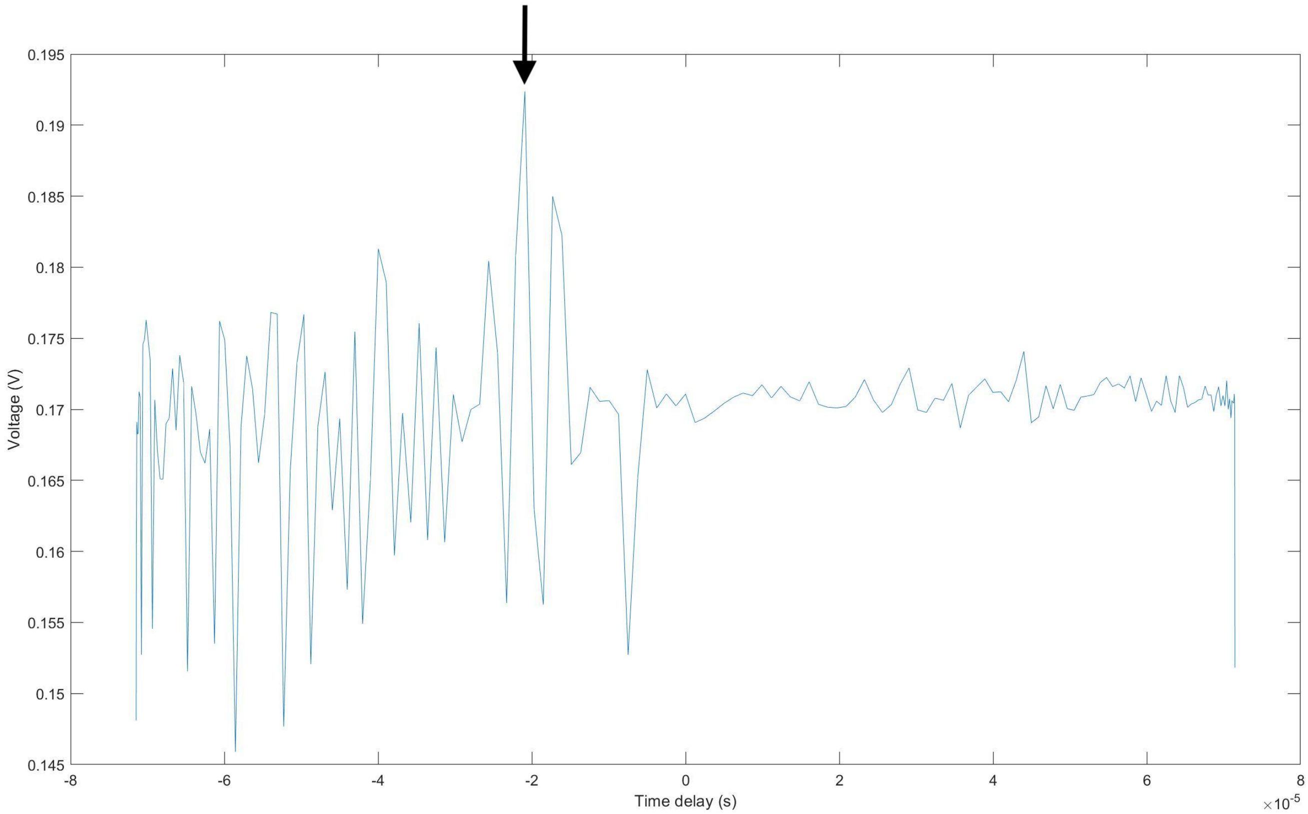

Figure 27: Focus on PWAS6. Signal arriving at receiver PWAS6 for different time delays. Time delay between PWAS1, PWAS2 and PWAS3 is constant, between PWAS1 and PWAS4 is variable. The arrow indicates the time delay where the phased array arrives at the receiver.

The time delays used for this method can be seen in table 9.

Table 9: Time delays found for iteration method

200 kHz	**To PWAS5**	**To PWAS6**	**To PWAS7**	**To PWAS8**
T0	0 s	0 s	0 s	0 s
T1	-8.93e-6 s	1.08e-5 s	2.06e-5 s	2.25e-5 s
T2	-3.37e-5 s	-1.66e-6 s	2.73e-5 s	3.90e-5 s
T3	-5.05e-5 s	-2.09e-5 s	1.61e-5 s	4.87e-5 s

When comparing these values to the ones found in table 8, the values in table 10 can be found. These values are the differences in percentage of table 9 with respect to table 8.

Table 10: Differences in percentage of the time delays used in the different methods

200 kHz	**To PWAS5**	**To PWAS6**	**To PWAS7**	**To PWAS8**
T0	0%	0%	0%	0%
T1	-6.97%	14.89%	18.39%	14.80%
T2	17.01%	176.67%	-5.86%	-3.94%
T3	1.41%	7.73%	-16.15%	-3.75%

The mean of the absolute values is 23.96% with a standard deviation of 48.45%. These values are acceptable; they significantly influence the outcome of the measurements. This difference will most likely be caused by the lack of omnidirectional waves. Consequentially, the wave propagation velocity of the plate is not constant between directions.

Using this method, the maximum amplitudes which can be seen in table 11 have been found. The underlined values are expected to be the largest, since these are the values received at the receivers when focused on.

Table 11: Maximum amplitude found when focusing on different PWAS at different receivers for iteration method

	Focus on 5	**Focus on 6**	**Focus on 7**	**Focus on 8**
Max amplitude at 5	<u>0.122 V</u>	0.172 V	0.138 V	0.0975 V
Max amplitude at 6	0.117 V	<u>0.192 V</u>	0.143 V	0.123 V
Max amplitude at 7	0.111 V	0.167 V	<u>0.161 V</u>	0.112 V
Max amplitude at 8	0.101 V	0.171 V	0.141 V	<u>0.127 V</u>

Analysis has shown that the maximum amplitudes found with this method are higher than the amplitudes discovered with the method used before, which was based on the time delays found with equation (1). The values are also largest at a receiver when this specific receiver is focused on. The steering of the phased array can thus be done using this iterating method.

5.4.3 TOF found values

Another method for creating a focused phased array is using the found time of flights and calculating how much longer it takes the wave signals to travel longer paths. By sending the wave signals that have to travel longer earlier than the wave signals that have to travel the shortest distance, the wave can arrive simultaneously at a focused receiver. Consequentially, superposition will occur.

The result of this method can be seen in figure 28. The other results can be seen in section A.2.8.

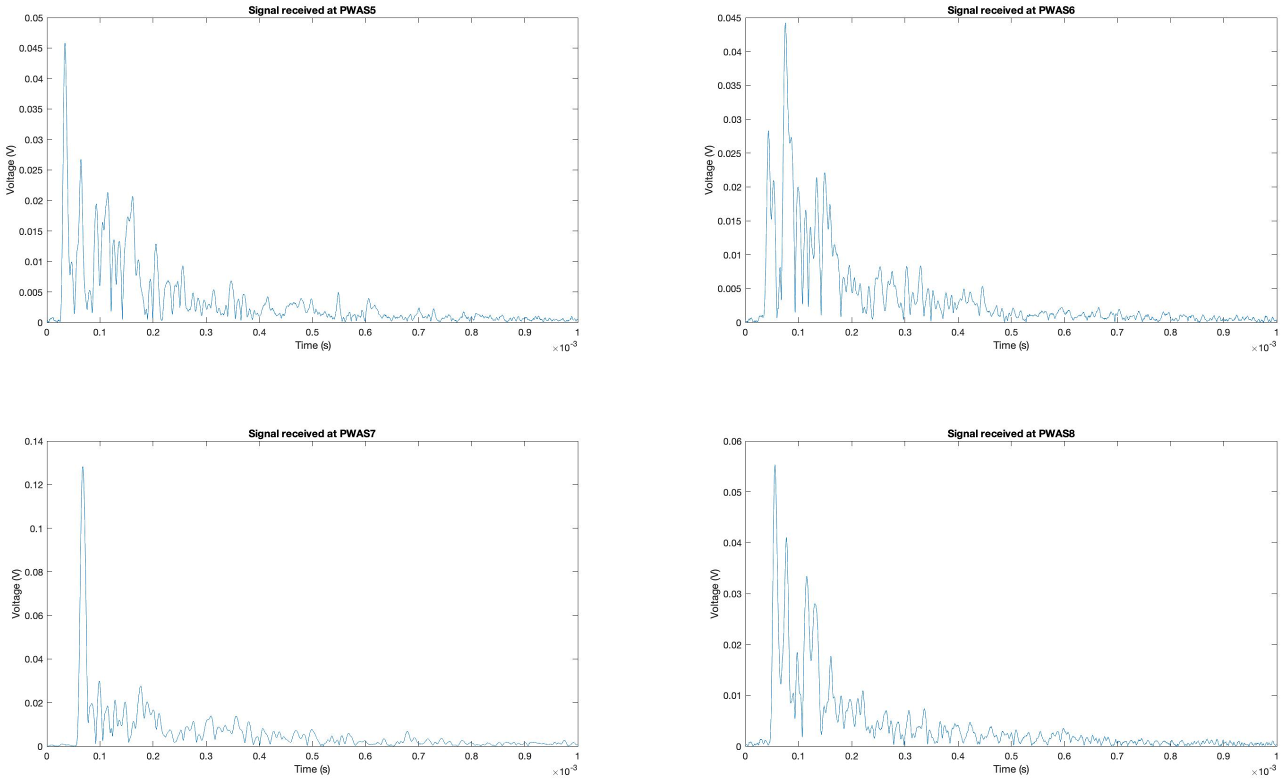

Figure 28: Signal arriving at receivers for TOF found time delays. Focus on PWAS7.

The amplitude of their largest peak can be seen in table 12.

Table 12: Maximum amplitude found when focusing on different PWAS at different receivers for TOF method

	Focus on 5	**Focus on 6**	**Focus on 7**	**Focus on 8**
Max amplitude at 5	0.0685 V	0.0450 V	0.0458 V	0.0460 V
Max amplitude at 6	0.0313 V	0.0775 V	0.0442 V	0.0502 V
Max amplitude at 7	0.0742 V	0.0940 V	0.128 V	0.0748 V
Max amplitude at 8	0.0552 V	0.0560 V	0.0553 V	0.0887 V

The values seen in this table 12 are generally lower than the previous established values in table 11. Especially for PWAS5 and PWAS6, the values found when focusing on the receiver are not largest at the receiver. These values are largest at PWAS7 and PWAS8.

This might potentially be the result of the lack of omnidirectional waves due to the composite material properties. Another issue could be the damage present in the plate. To find out exactly why the focusing does not behave as expected, future complementary research is needed.

5.4.4 Damage detection

The quasi-isotropic material properties of the composite plate cause the plate to have different wave behaviour in different directions. Thus, differences when a signal has come across damage versus when it has not come across damage cannot be identified. The wave signals behave differently when travelling in another direction. Therefore, two different paths, even if they are the same length, cannot be compared well enough to find more information on the effect of damage being present in a composite plate.

To solve this problem, measurements should be taken first on the plate without damage. Afterwards, the impact damage can be created on the plate. Finally, the measurements with damage can be conducted.

6 Discussion

The measurements have shown some promising results. Nevertheless, some drawbacks of the study should be taken into account.

Firstly, the determination method regarding the time of flights for both the S_0 and A_0 mode can be questioned. In this research, the time difference between a peak of the actuation signal and a peak of the arriving signal at the receiver were compared. For the S_0 mode, this was usable. Another method to provide similar data is finding the correlation between the sent and received signal, perhaps with higher accuracy. The A_0 mode was not detectable due to too much attenuation. The previously mentioned method could possibly resolve this. Another suggestion will be presented in the recommendations below.

Furthermore, the performed composite plate measurements were assumed to be quasi-isotropic. This implies that the plate has approximately the same material properties in all directions. Thus, the waves propagate at the same velocity in all directions. However, these omnidirectional waves do not occur, partly due to the presence of the stiffeners. Consequently, equation (1) could not be used. Instead, individual experimental-based time delays are preferable.

Thirdly, several side lobes occur when the phased array beam is focused in certain directions. Quite some energy is lost to the side lobes because of this, which influences the resolution of the signal. The measurement setup of this research complicates preventing these side lobes. Therefore, the setup might benefit from some adaptations, discussed in the recommendations.

Alternatively, the side lobes might have been created due to malfunctioning of PWAS2. Since the results have shown that the actuator sends a signal of relatively smaller amplitude, constructive and destructive interference might have behaved different due to this. This did not influence the focus direction however.

Finally, it is left undecided how the wave signals are affected by the damage. The measurements were conducted on a plate with impact damage present, leaving no measurements of the plate without damage available.

6.1 Recommendations

Future research can be taken into several directions to explore the possibilities of using focused phased array wave beams for damage detection.

First of all, using a new setup in which the actuators are located closer to each other could provide some interesting results. Fewer side lobes are expected, thus enlarging the amplitude of the main lobe.

Additionally, a setup in which the travelled paths are shortened could also benefit future research. Less attenuation could occur in the A_0 mode signal. Therefore, it might be possible to create a phased array based on the A_0 mode.

Another aspect that could be adjusted is iterating over several time delays, as partly undertaken in this research. In this research, a peak was found and the time delay of this peak was made constant. Then there was iterated over the time delay between two other actuators. Afterwards, an iteration was done over the time delay between two other actuators. This method could be further exploited by making all time delays variables simultaneously and starting the iteration at that moment. With this method, a larger amplitude of the signal could be found in the direction of focusing.

Finally, it would be interesting to compare the results found on a path of a damaged and undamaged plate. As written before, this is not possible with the current setup.

7 Conclusion

In this thesis, possibilities on how the observation of damage in a composite plate using a phased array measuring method were researched.

Most notably, it was discovered that the resolution of the signals can be enhanced by focusing the phased array beam on the receiver, such that a signal with a high amplitude can be measured. Thus, more information can be extracted from the signal. Furthermore, the frequencies used influence the research. A too high frequency (close to 250kHz) will lower the resolution of the signal received.

Secondly, the used frequencies are 150kHz and 200kHz. 200kHz has already shown promising results in previous research and the theory has demonstrated that 150kHz is also suitable for use. For both these frequencies, only the S_0 and A_0 mode will be present. To detect the S_0 mode, the 200kHz frequency is best to use. For the A_0 mode, this is the 150kHz frequency.

The focused area of the phased array can be changed by adapting the time delay of when the different actuation signals are sent. This can be done by e.g. using equation (1), but this research has shown that it is better to use individual time delays. When doing so, the amplitude of the arriving signal is larger and thus the focusing can be done more accurately. Several methods to implement individual time delays exist. Firstly, different time delays can be iterated over, making a phased array possible. Secondly, the different recorded time of flights can be used to ensure the interference occurs at the receiver. This first method provided the best focused signals, which also had larger amplitudes than all the other conducted experiments in this research.

Retrieving information about the impact damage was not possible, since no measurements of the plate without damage could be conducted. Two different paths of the same length could not be compared due to the waves travelling at different velocities in the directions of the setup. This influenced the analysis of the results.

All in all, a phased array can be created using actuators with varying time delays. It is best to do this through experiments, since the quasi-isotropic material properties of the composite plate affect the location where the focusing of the phased array will occur. Therefore, experimentally based individual time delays are most suitable to use. This will enhance the observability of the signal in a chosen direction in further measurements.

References

[1] ScienceDirect. *Composite Material*. URL: https://www.sciencedirect.com/topics/chemistry/composite-material. (accessed: 12.03.2021).

[2] Justin Hale. "Boeing 787 from the Ground Up". In: *Aero* (2006). URL: https://www.boeing.com/commercial/aeromagazine/articles/qtr_4_06/AERO_Q406_article4.pdf.

[3] Nikhil P. Raut, A.b. Kolekar, and S.l. Gombi. "Optimization techniques for damage detection of composite structure: A review". In: *Materials Today: Proceedings* 45 (Feb. 2021), pp. 4830–4834. DOI: 10.1016/j.matpr.2021.01.295. URL: https://www.sciencedirect.com/science/article/pii/S2214785321003849.

[4] Ye Lu Zhonggin Su Lin Ye. "Guided Lamb waves for identification of damage in composite structures: A review". In: *Journal of Sound and Vibration* 295.3-5 (2006), pp. 753–780. ISSN: 0022-460X. DOI: 10.1533/9780857099136.86. URL: https://www.sciencedirect.com/science/article/pii/S0022460X0600109X.

[5] Marek Barski, Piotr Kedziora, Aleksander Muc, and Paweł Romanowicz. "Structural Health Monitoring (SHM) Methods in Machine Design and Operation". In: *Archive of Mechanical Engineering* 61 (Dec. 2014). DOI: 10.2478/meceng-2014-0037. URL: https://www.researchgate.net/publication/276336620_Structural_Health_Monitoring_SHM_Methods_in_Machine_Design_and_Operation.

[6] Pawel Malinowski, Tomasz Wandowski, Iirina Trendafilova, and Wieslaw Ostachowicz. "A Phased Array-based Method for Damage Detection and Localization in Thin Plates". In: *Structural Health Monitoring-an International Journal - STRUCT HEALTH MONIT* 8 (2008), pp. 5–15. DOI: 10.1177/1475921708090569. URL: https://www.researchgate.net/publication/239405286_A_Phased_Array-based_Method_for_Damage_Detection_and_Localization_in_Thin_Plates.

[7] Giovanni Selamat. "Damage monitoring of Carbon Fibre Reinforced Polymer utilizing Ultrasonic Guided Waves Phased Array method". In: (2020). BSc thesis.

[8] Abdullah Cahit Karaoglanli Dervis Ozkan Mustafa Sabri Gok. *Engineering Design Applications III*. Advanced Structured Materials. Springer, Cham, 2020. ISBN: 978-3-030-39062-4.

[9] DragonPlate. *Carbon Fibre 101: What do Isotropic, Quasi-Isotropic, and Anisotropic Mean?* URL: https://dragonplate.com/carbon-fiber-101-what-do-isotropic-quasi-isotropic-and-anisotropic-mean. (accessed: 16.03.2021).

[10] Qing-Qing Ni Junjie Chang Changliang Zheng. "The ultrasonic wave propagation in composite material and its characteristic evaluation," in: *Composite Structures* 75.1-4 (Apr. 2006), pp. 5–15. DOI: https://doi.org/10.1016/j.compstruct.2006.04.040. URL: https://www.sciencedirect.com/science/article/pii/S0263822306001711?via%5C%3Dihub.

[11] Guoyi Li, Rajesh Kumar Neerukatti, and Aditi Chattopadhyay. "Ultrasonic guided wave propagation in composites including damage using high-fidelity local interaction simulation". In: *Journal of Intelligent Material Systems and Structures* 29 (Sept. 2017), p. 1045389X1773065. DOI: 10.1177/1045389X17730659. URL: https://www.researchgate.net/publication/319919553_Ultrasonic_guided_wave_propagation_in_composites_including_damage_using_high-fidelity_local_interaction_simulation.

[12] Keith Worden, Charles R. Farrar, Graeme Manson, and Gyuhae Park. "The Fundamental Axioms of Structural Health Monitoring". In: *Proceedings: Mathematical, Physical and Engineering Sciences* 463.2082 (2007), pp. 1639–1664. ISSN: 13645021. DOI: 10.1098/rspa.2007.1834. URL: http://www.jstor.org/stable/20209268.

[13] Olympus. *Wave Propagation*. URL: https://www.olympus-ims.com/en/ndt-tutorials/flaw-detection/wave-propagation/. (accessed: 09.03.2021).

[14] L. YU, Giola Santoni, B. XU, W. LIU, and Victor Giurgiutiu. “Piezoelectric wafer active sensors for in situ ultrasonic-guided wave SHM”. In: *Fatigue Fracture of Engineering Materials Structures* 31 (Aug. 2008), pp. 611–628. DOI: 10.1111/j.1460-2695.2008.01256.x. URL: https://www.researchgate.net/publication/227604796_Piezoelectric_wafer_active_sensors_for_in_situ_ultrasonic-guided_wave_SHM.

[15] Y. Sharma. *Rain erosion damage assessment using ultrasonics*. MSc thesis. May 2020. URL: http://essay.utwente.nl/81320/.

[16] Zhongqing Su and Lin Ye. “Fundamentals and Analysis of Lamb Waves”. In: *Lecture Notes in Applied and Computational Mechanics* 48 (Jan. 2009). DOI: 10.1007/978-1-84882-784-4_2. URL: https://www.researchgate.net/publication/251341822_Fundamentals_and_Analysis_of_Lamb_Waves.

[17] H. Sohn Y.K. An M.K. Kim. “4 - Piezoelectric transducers for assessing and monitoring civil infrastructures”. In: *Sensor Technologies for Civil Infrastructures* 55.1 (2014), pp. 86–120. DOI: 10.1533/9780857099136.86. URL: https://www.sciencedirect.com/science/article/pii/B9780857094322500048.

[18] Victor Giurgiutiu. “Structural health monitoring with piezoelectric wafer active sensors - predictive modeling and simulation”. In: 2.3 (2010), pp. 31–44. ISSN: 2066-8201. DOI: 10.1533/9780857099136.86. URL: https://www.researchgate.net/publication/275554983_Structural_health_monitoring_with_piezoelectric_wafer_active_sensors_-_predictive_modeling_and_simulation.

[19] Kanji Ono and A. Gallego. “Attenuation of Lamb waves in CFRP plates”. In: *J Acoust Emission* 30 (Jan. 2012), pp. 109–123. URL: https://www.researchgate.net/publication/285253240_Attenuation_of_Lamb_waves_in_CFRP_plates.

[20] Morteza Tabatabaeipour, Jan Hettler, Steven Delrue, and Koen Van Den Abeele. “Reconstruction Algorithm for Probabilistic Inspection of Damage (RAPID) in Composites”. In: Oct. 2014.

[21] Lingyu Yu and Victor Giurgiutiu. “In-situ Optimized PWAS Phased Arrays For Lamb Wave Structural Health Monitoring”. In: *Journal of Mechanics of Materials and Structures* 2.3 (2007). DOI: 10.2140/jomms.2007.2.459. URL: https://msp.org/jomms/2007/2-3/jomms-v2-n3-p04-p.pdf.

[22] Olympus. *Phased Pulsing and Its Effects*. URL: https://www.olympus-ims.com/en/ndt-tutorials/transducers/generating/. (accessed: 23.04.2021).

[23] Gerhard Mook, Christian Willberg, Ulrich Gabbert, and Jürgen Pohl. “Lamb wave mode conversion in CFRP plates”. In: Oct. 2014. DOI: 10.13140/2.1.3372.4161. URL: https://www.researchgate.net/publication/266477491_Lamb_wave_mode_conversion_in_CFRP_plates.

[24] Christian Willberg, Gerhard Mook, Ulrich Gabbert, and Jürgen Pohl. “The Phenomenon of Continuous Mode Conversion of Lamb Waves in CFRP Plates”. In: *Smart Materials and Structures* 21 (June 2012), p. 075022. DOI: 10.1088/0964-1726/21/7/075022. URL: https://www.researchgate.net/publication/231051044_The_Phenomenon_of_Continuous_Mode_Conversion_of_Lamb_Waves_in_CFRP_Plates.

[25] Richard Loendersloot. “SHM of Skin-Stiffener Composite Structure Using Acousto-Ultrasonics and PWAS”. In: Sabbatical Research Project. 2016.

A Appendix

A.1 Measurement steps

A.1.1 Measuring time of flight (TOF)

1. Turn on the National Instruments chassis.
2. Open the Phased Array file in LabVIEW.
3. Set the actuation frequency to 150 kHz.
4. Set the actuation signal amplitude to 10 V.
5. Set the number of cycles produced by the actuation signal to 3.5.
6. Set the number of averages taken for the measurement to 10.
7. Set the measurement duration time to 1 s.
8. Start with one actuating transponder (in this case PWAS 1). Therefore, disconnect the analog output of the other actuating transponders on the National Instruments chassis.
9. Start the Phased Array program in LabVIEW.
10. Save the measurements once finished.
11. Repeat steps 8-10 for the other three actuating transponders.
12. Now repeat steps 3-11 for the other actuation frequency, which is 200 kHz.

When analysing the data found with these measurements, it should be taken into account that the S_0 mode of the wave signal travels at a higher speed than the A_0 mode of the wave signal. Therefore, two different time of flights will be obtained.

A.1.2 Measuring phased arrays

1. Turn on the National Instruments chassis.
2. Open the Phased Array file in LabVIEW.
3. Set the actuation frequency to 150 kHz.
4. Set the actuation signal amplitude to 10 V.
5. Set the number of cycles produced by the actuation signal to 3.5.
6. Set the number of averages taken for the measurement to 10. (Note: only for the iteration method this number is 4).
7. Set the measurement duration time to 1 s.
8. Input the already obtained TOF data from the previous measurement section. Start with the time of flights of the S_0 mode. Thereby, choose which receiving PWAS the phased array focuses on. The TOF data should be taken for the different actuating transponders to this chosen receiving PWAS.
9. Start the Phased Array program in LabVIEW.
10. Save the measurements once finished.

11. Repeat steps 8-10, but now use the time of flights obtained for the A_0 mode of the wave signal.

12. Repeat steps 8-11 for the other three receiving PWAS.

13. Repeat steps 3-11 for the other actuation frequency, being 200 kHz.

A.2 Results

A.2.1 Actuation signals

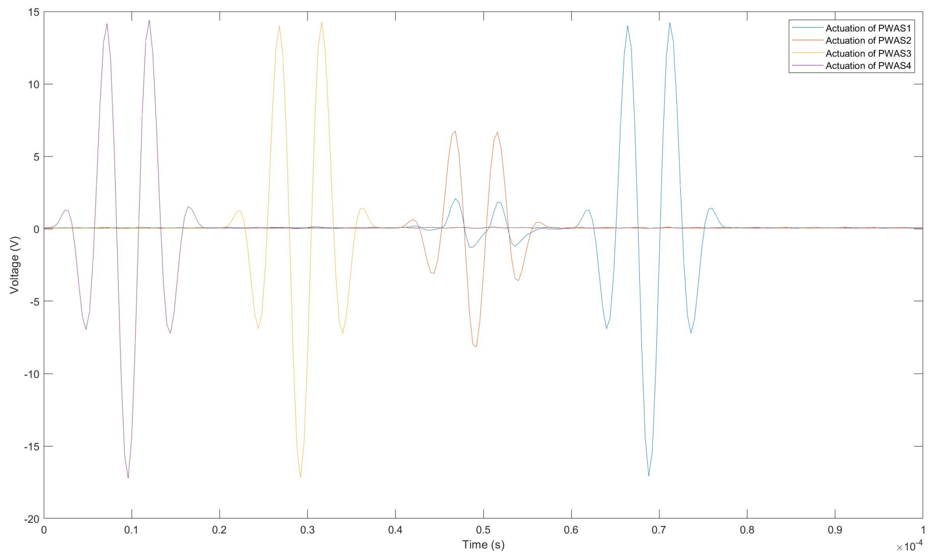

Figure 29: Actuation signals at a frequency of 200kHz.

A.2.2 Time of flight: S_0 mode

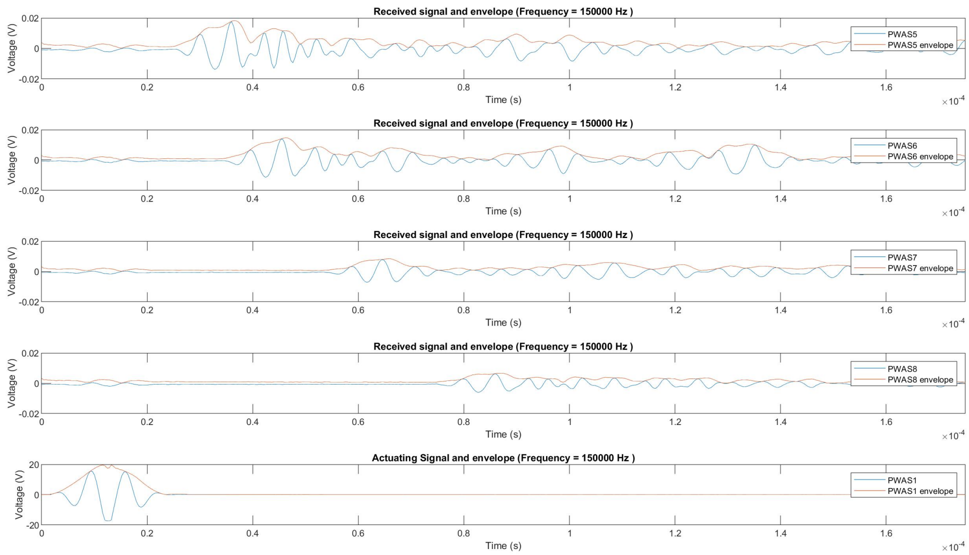

Figure 30: S_0 time of flight measurement with PWAS1 as actuator at 150kHz.

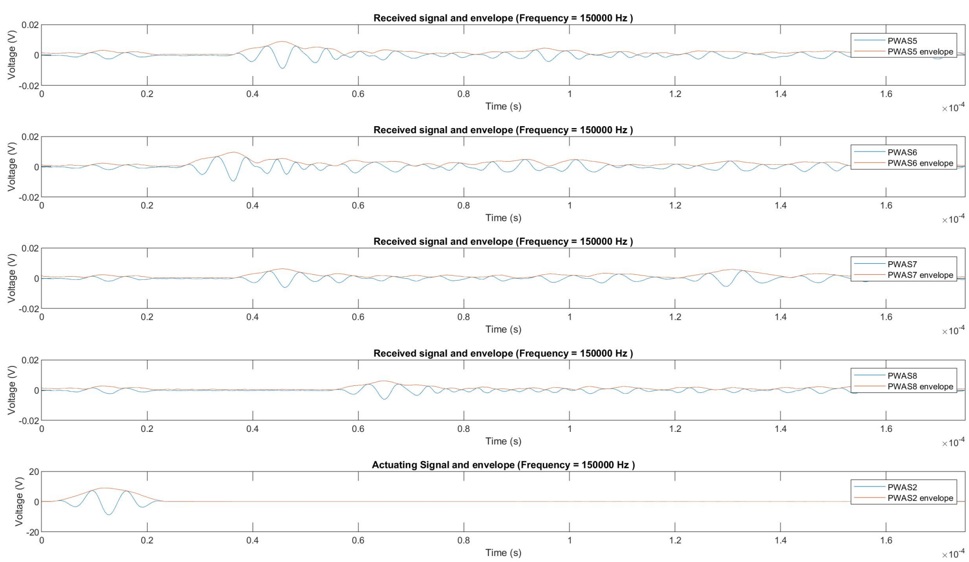

Figure 31: S_0 time of flight measurement with PWAS2 as actuator at 150kHz.

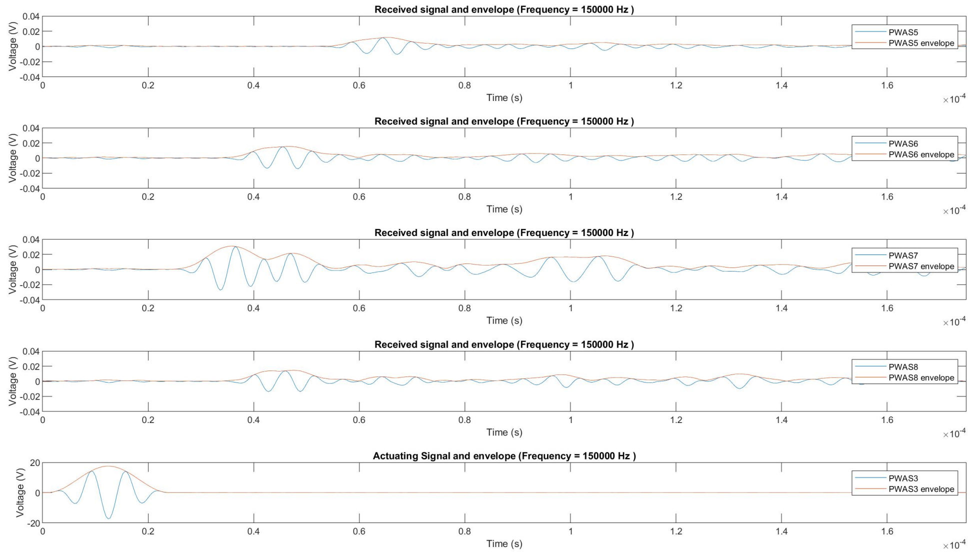

Figure 32: S_0 time of flight measurement with PWAS3 as actuator at 150kHz.

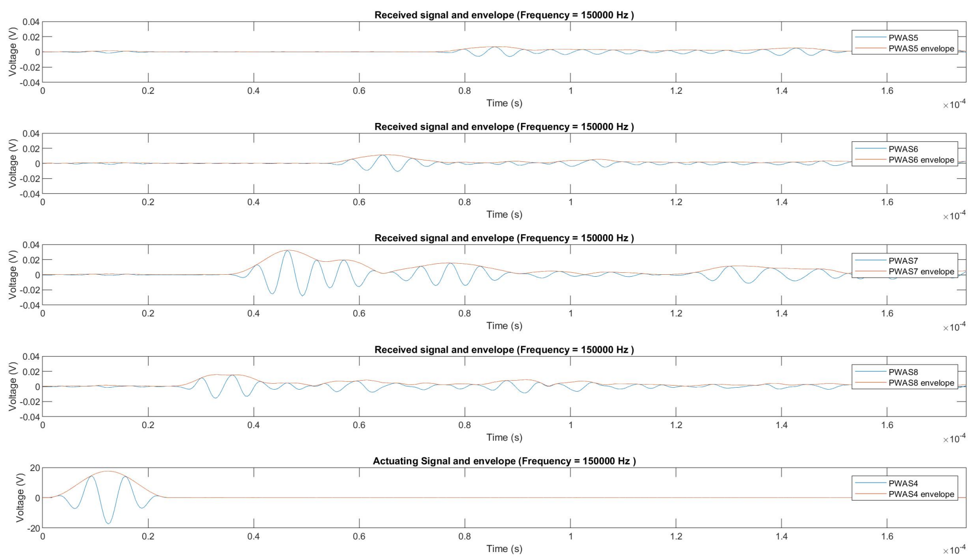

Figure 33: S_0 time of flight measurement with PWAS4 as actuator at 150kHz.

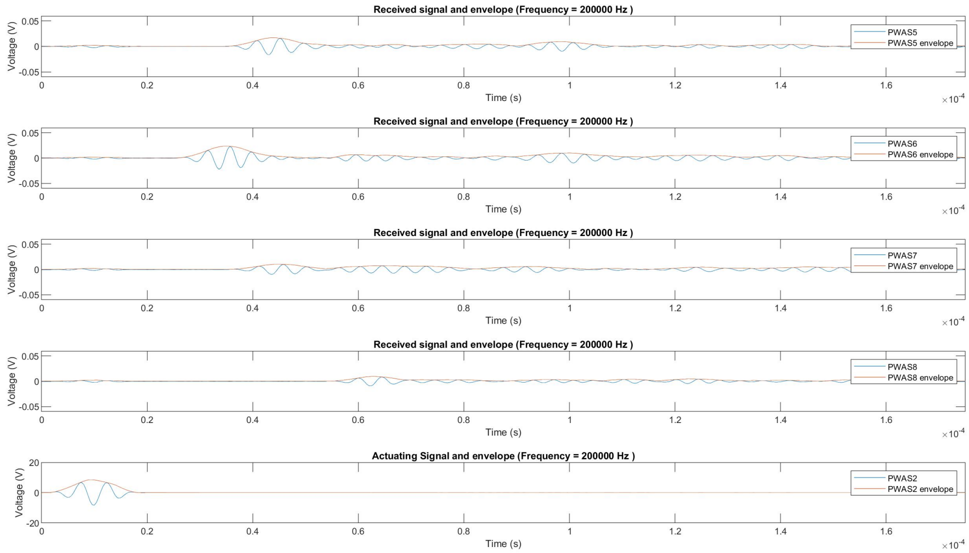

Figure 34: S_0 time of flight measurement with PWAS2 as actuator at 200kHz.

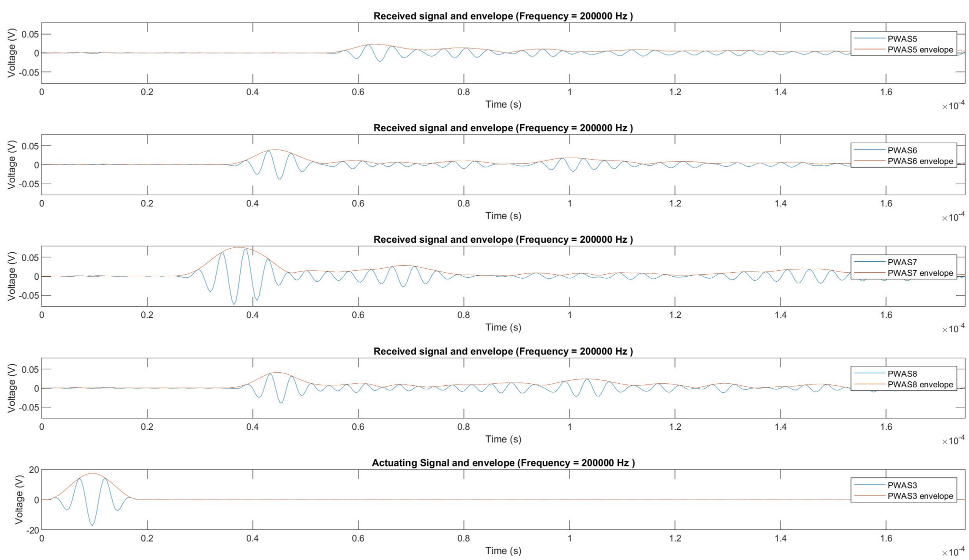

Figure 35: S_0 time of flight measurement with PWAS3 as actuator at 200kHz.

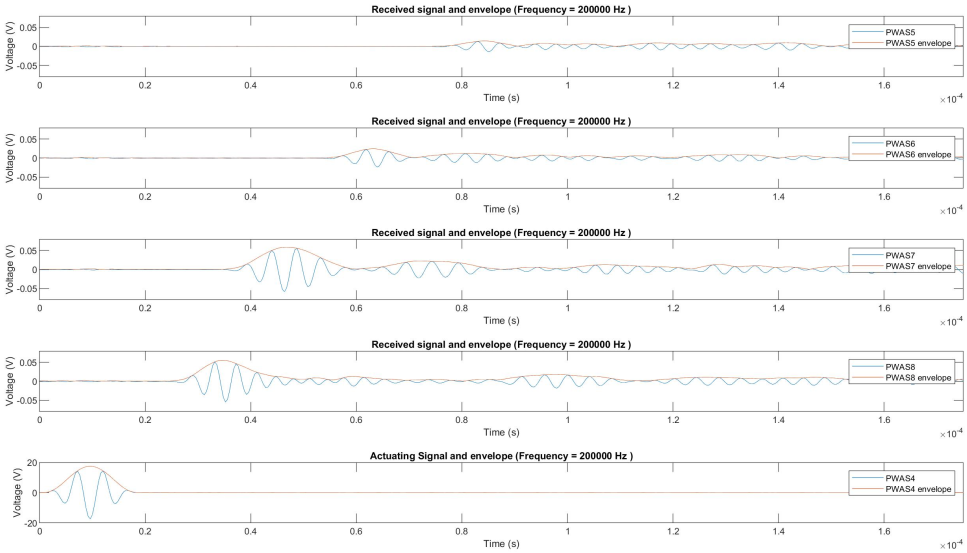

Figure 36: S_0 time of flight measurement with PWAS4 as actuator at 200kHz.

A.2.3 Time of flight: A_0 mode

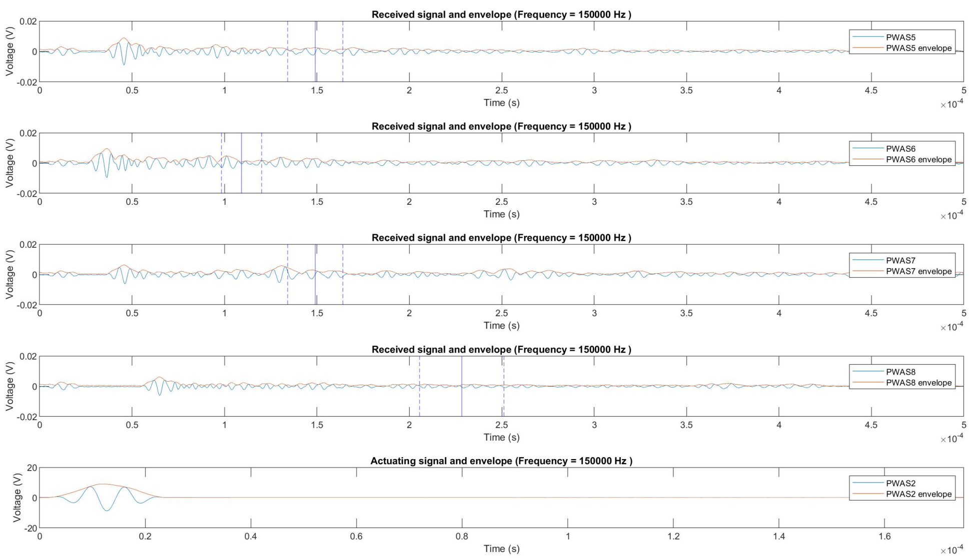

Figure 37: A_0 time of flight analysis, with PWAS2 as actuator at 150kHz.

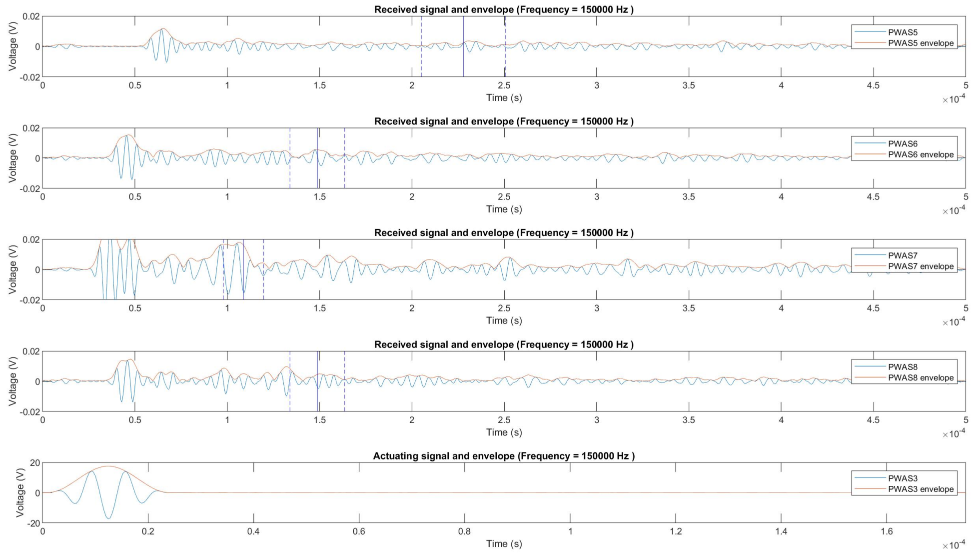

Figure 38: A_0 time of flight analysis, with PWAS3 as actuator at 150kHz.

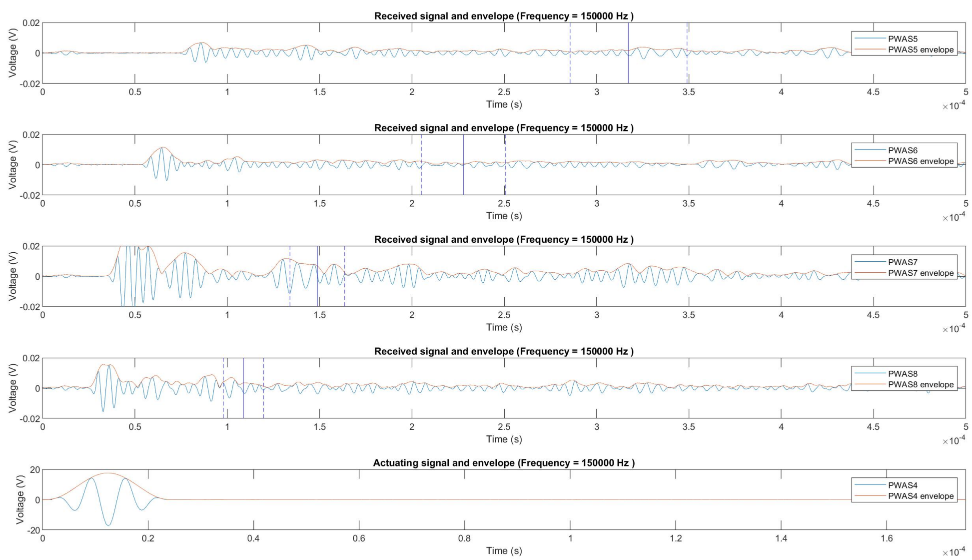

Figure 39: A_0 time of flight analysis, with PWAS4 as actuator at 150kHz.

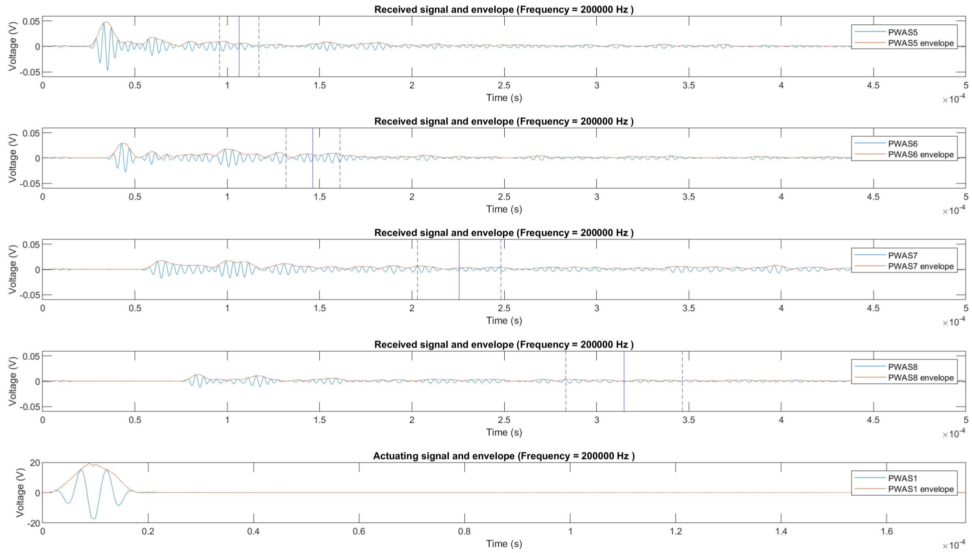

Figure 40: A_0 time of flight analysis, with PWAS1 as actuator at 200kHz.

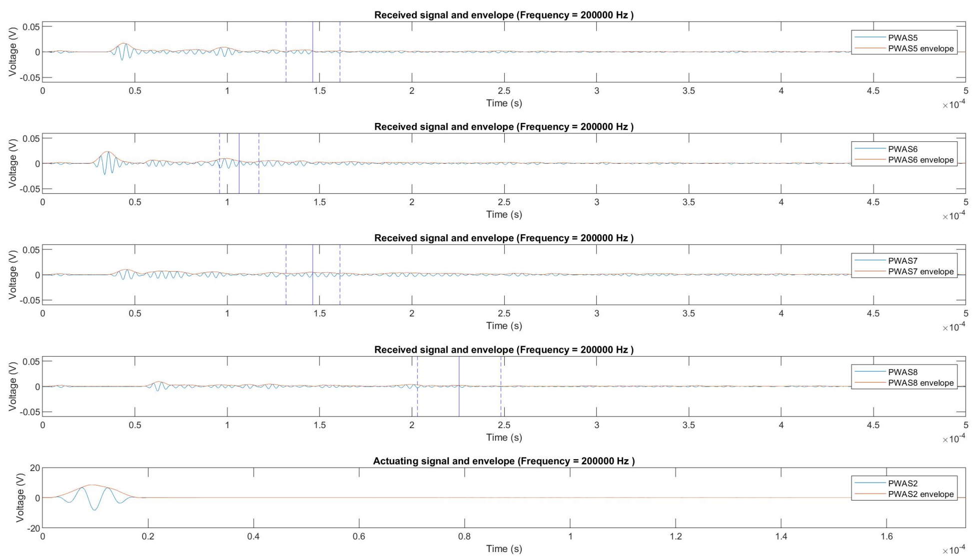

Figure 41: A_0 time of flight analysis, with PWAS2 as actuator at 200kHz.

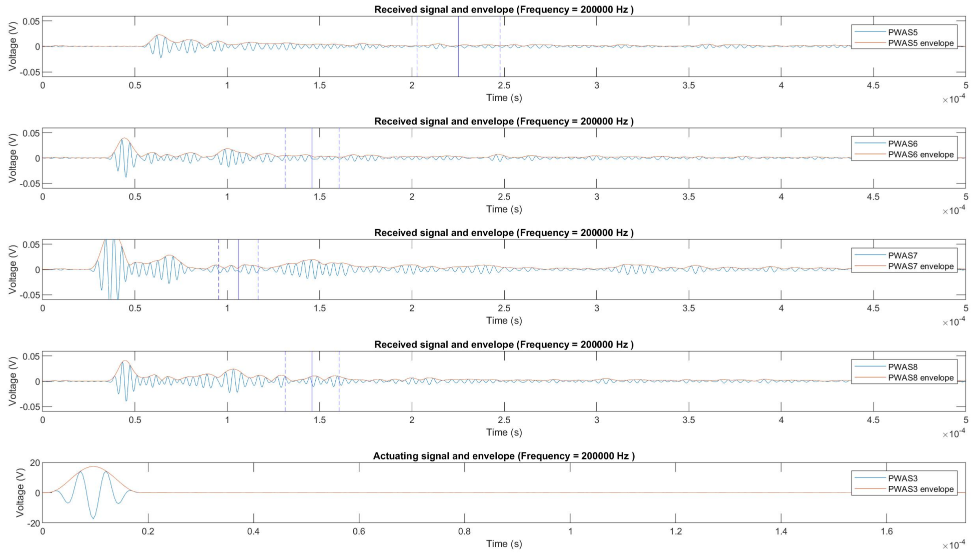

Figure 42: A_0 time of flight analysis, with PWAS3 as actuator at 200kHz.

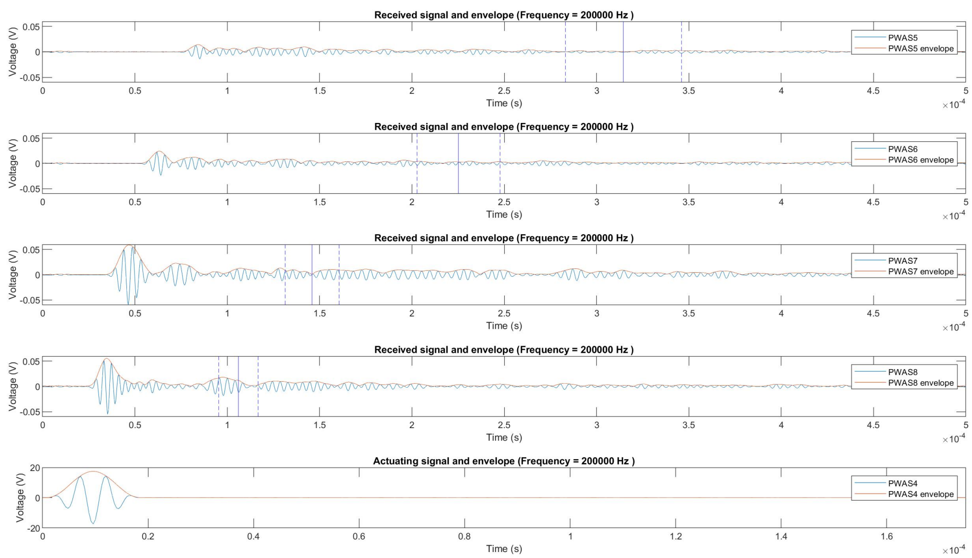

Figure 43: A_0 time of flight analysis, with PWAS4 as actuator at 200kHz.

A.2.4 Phased array (theoretical time delays): superposition of signal

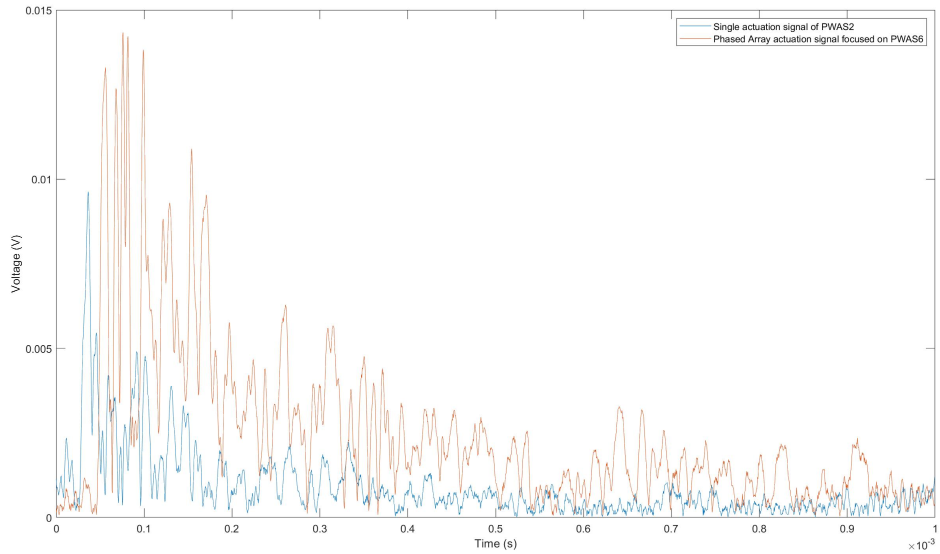

Figure 44: Single actuation of PWAS2 in comparison to phased array focused on PWAS6 at 150kHz.

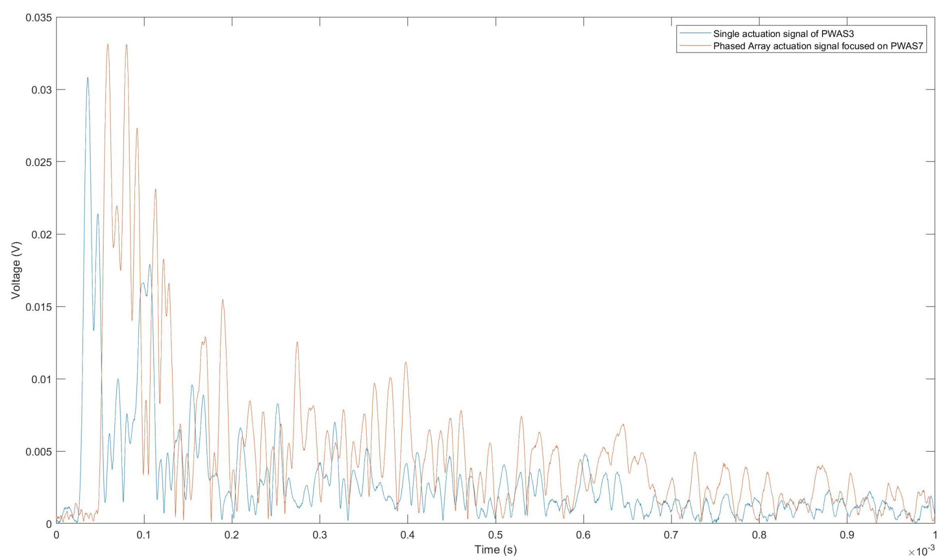

Figure 45: Single actuation of PWAS3 in comparison to phased array focused on PWAS7 at 150kHz.

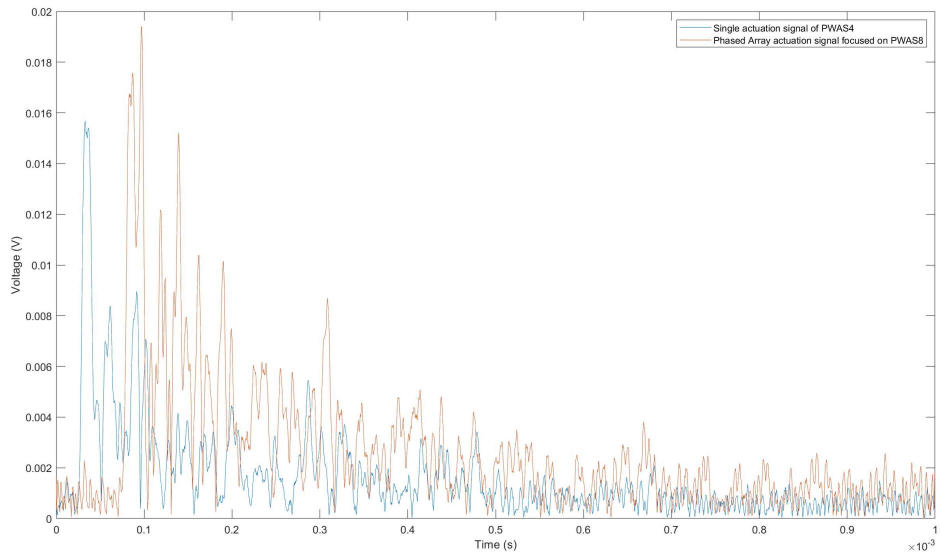

Figure 46: Single actuation of PWAS4 in comparison to phased array focused on PWAS8 at 150kHz.

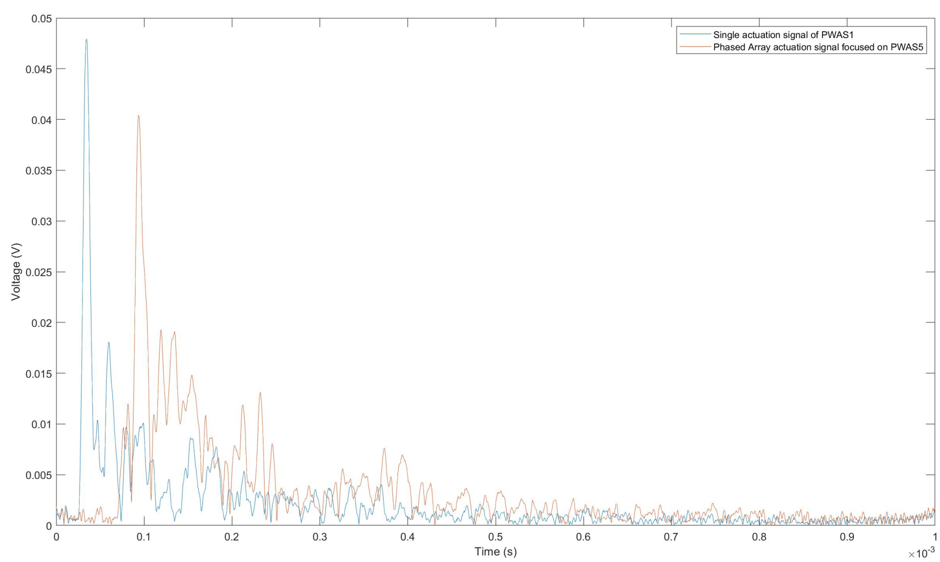

Figure 47: Single actuation of PWAS1 in comparison to phased array focused on PWAS5 at 200kHz.

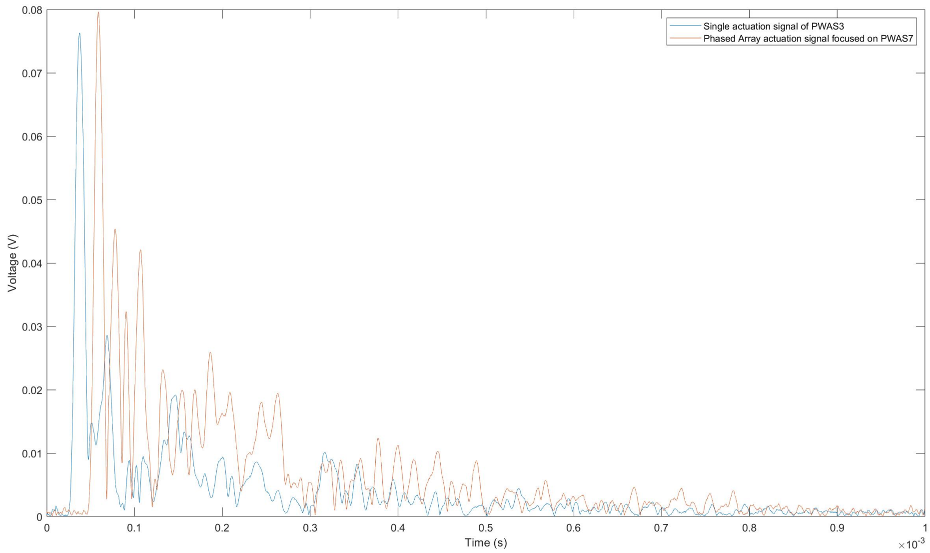

Figure 48: Single actuation of PWAS3 in comparison to phased array focused on PWAS7 at 200kHz.

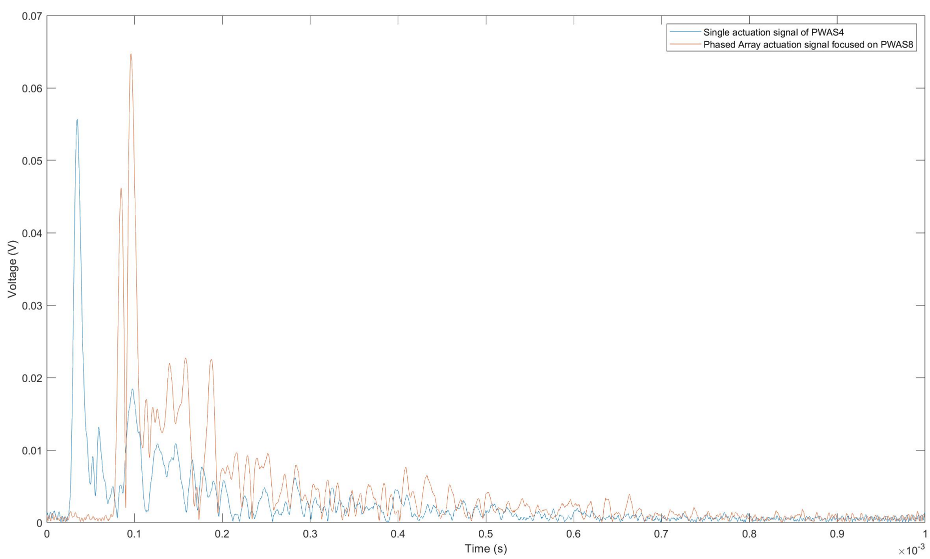

Figure 49: Single actuation of PWAS4 in comparison to phased array focused on PWAS8 at 200kHz.

A.2.5 Phased array (theoretical time delays): focusing of signal

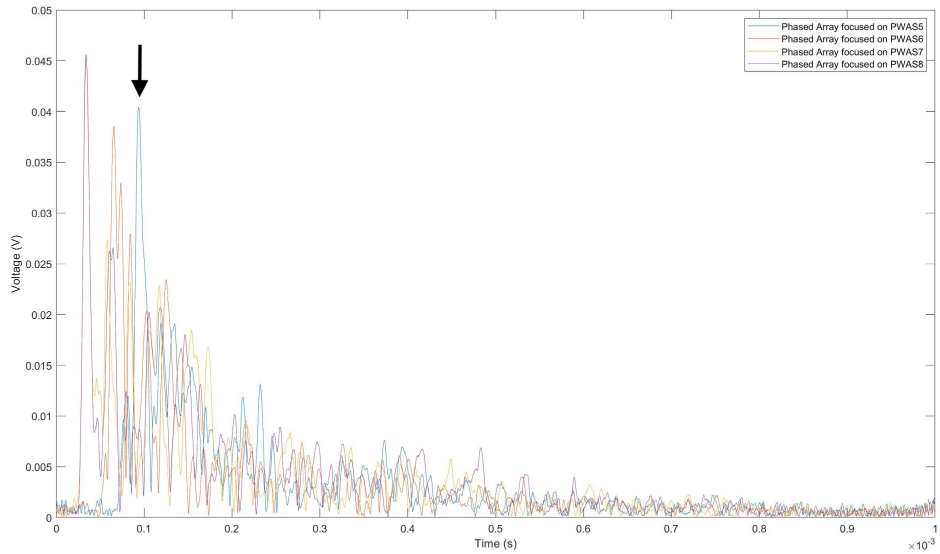

Figure 50: Signal received at PWAS5 when focusing on different PWAS. The arrow indicates the peak of the signal of the PWAS which is expected to be largest.

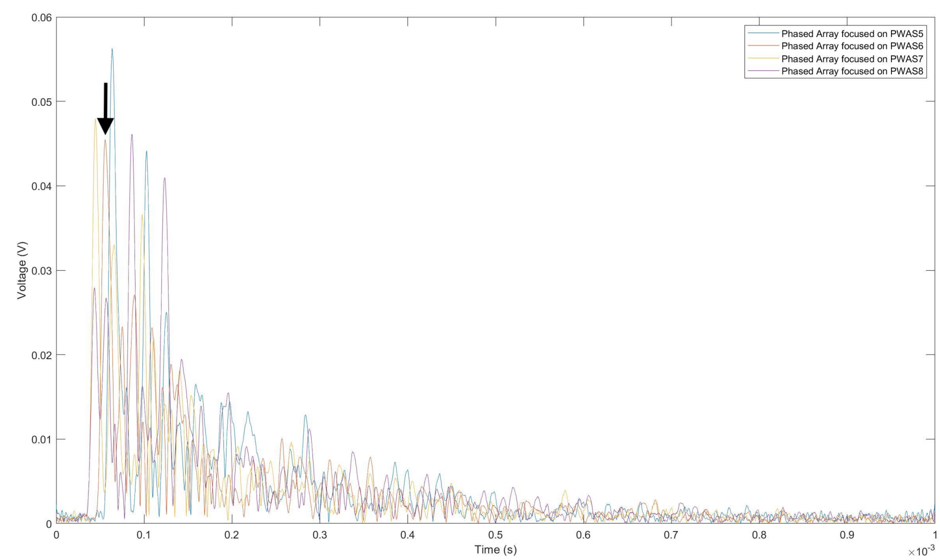

Figure 51: Signal received at PWAS6 when focusing on different PWAS. The arrow indicates the peak of the signal of the PWAS which is expected to be largest.

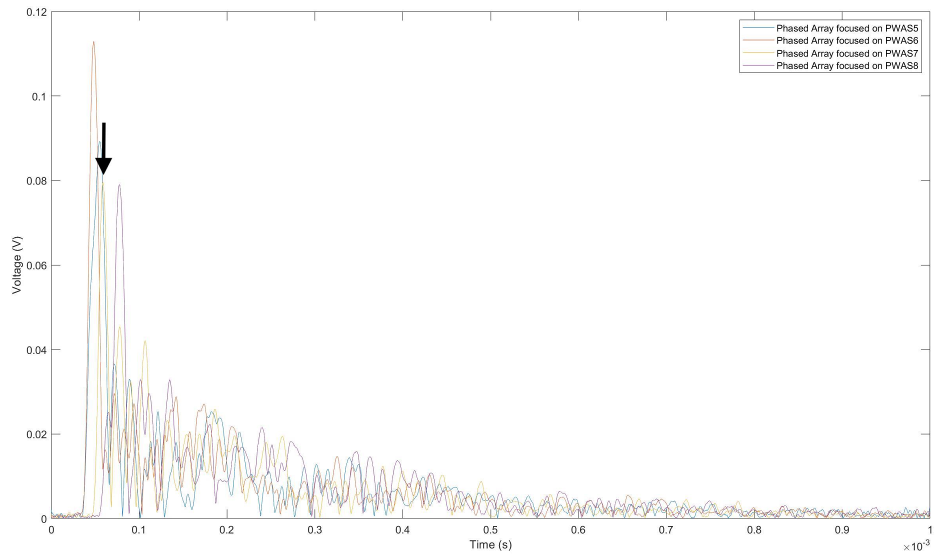

Figure 52: Signal received at PWAS7 when focusing on different PWAS. The arrow indicates the peak of the signal of the PWAS which is expected to be largest.

A.2.6 Phased array (experimental time delays): iterating over time delay (3D plots)

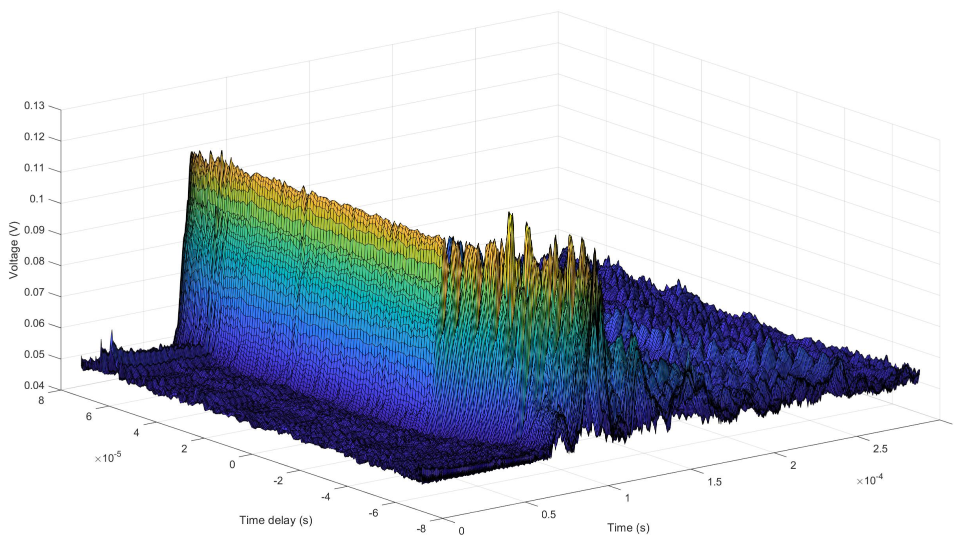

Figure 53: Signal received at PWAS5 for phased array focused on PWAS5, iterating over the time delay between PWAS1 and PWAS4. Other time delays are set to certain value based on previous measurements.

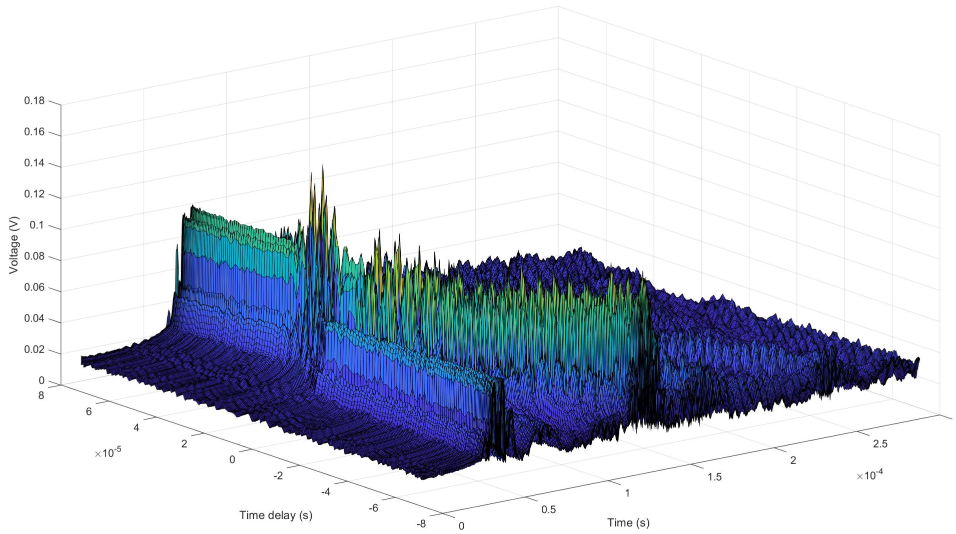

Figure 54: Signal received at PWAS7 for phased array focused on PWAS7, iterating over the time delay between PWAS1 and PWAS4. Other time delays are set to certain value based on previous measurements.

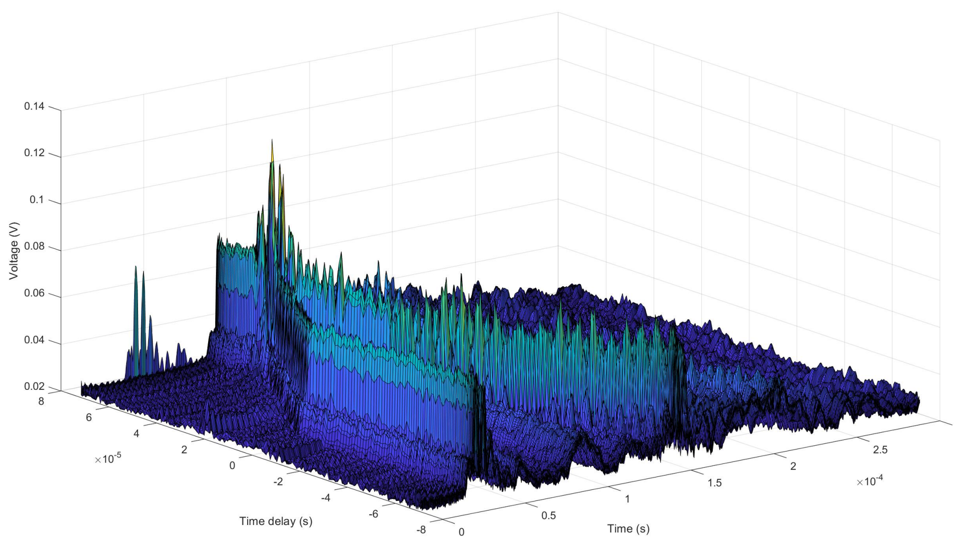

Figure 55: Signal received at PWAS8 for phased array focused on PWAS8, iterating over the time delay between PWAS1 and PWAS4. Other time delays are set to certain value based on previous measurements.

A.2.7 Phased array (experimental time delays): iterating over time delay (building PA)

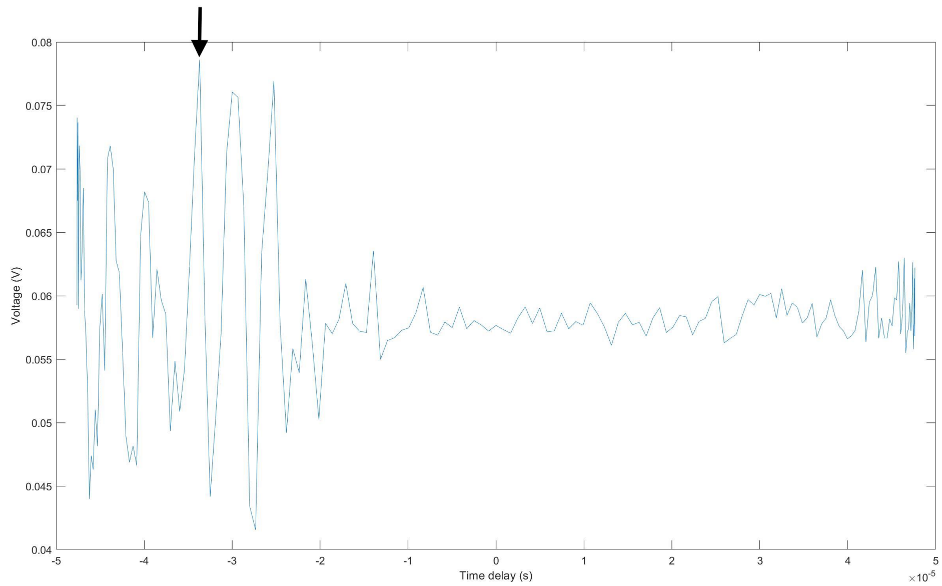

Figure 56: Focus on PWAS5. Signal arriving at receiver PWAS5 for different time delays. Time delay between PWAS1 and PWAS2 is constant, between PWAS1 and PWAS3 is variable. The arrow indicates the time delay where the phased array arrives at the receiver.

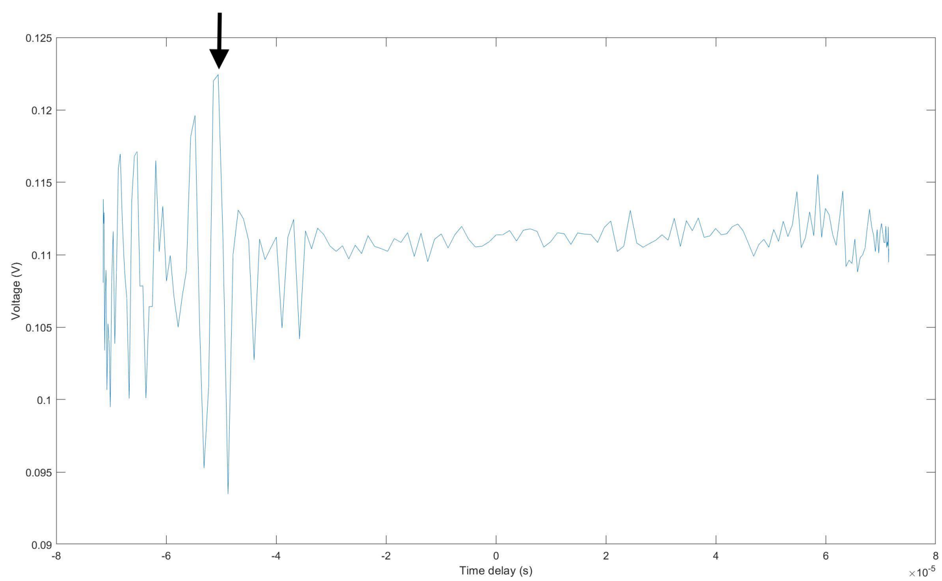

Figure 57: Focus on PWAS5. Signal arriving at receiver PWAS5 for different time delays. Time delay between PWAS1, PWAS2 and PWAS3 is constant, between PWAS1 and PWAS4 is variable. The arrow indicates the time delay where the phased array arrives at the receiver.

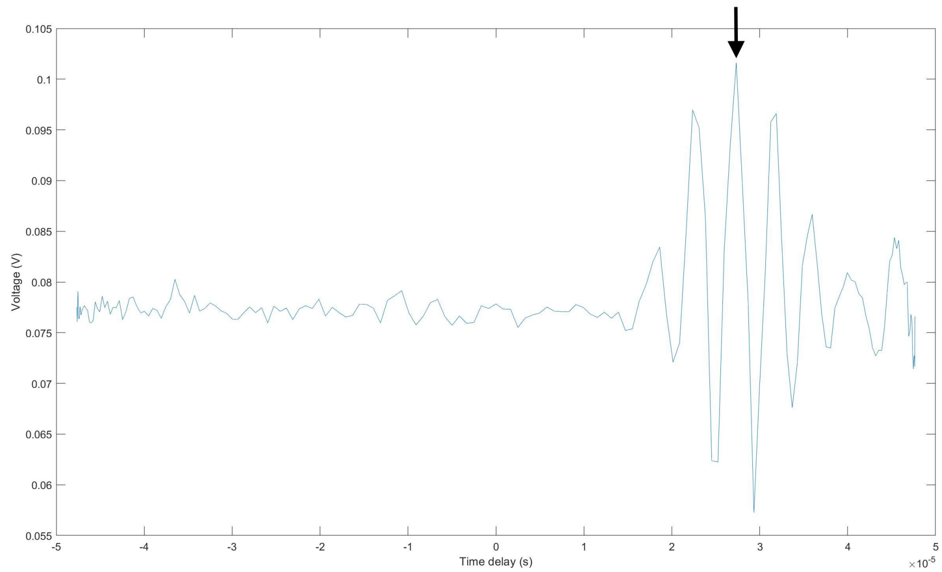

Figure 58: Focus on PWAS7. Signal arriving at receiver PWAS7 for different time delays. Time delay between PWAS1 and PWAS2 is constant, between PWAS1 and PWAS3 is variable. The arrow indicates the time delay where the phased array arrives at the receiver.

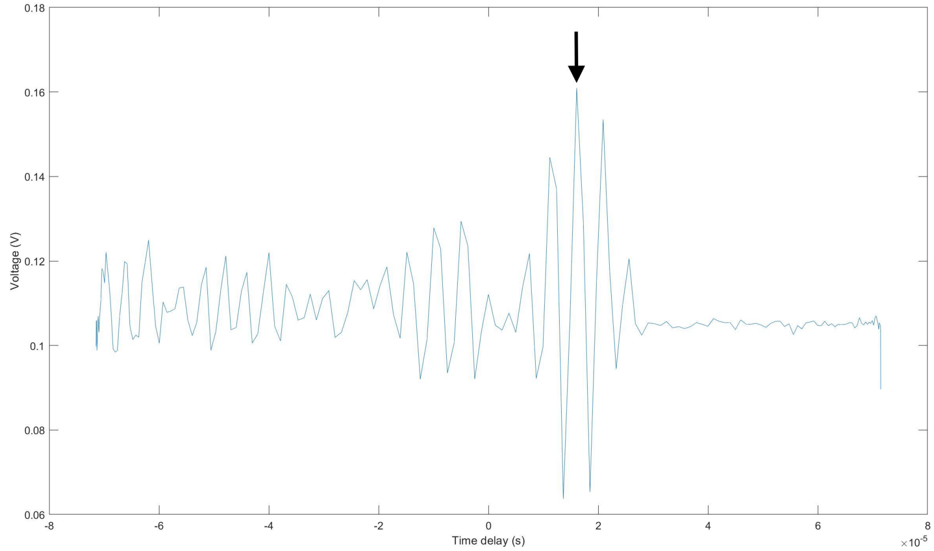

Figure 59: Focus on PWAS7. Signal arriving at receiver PWAS7 for different time delays. Time delay between PWAS1, PWAS2 and PWAS3 is constant, between PWAS1 and PWAS4 is variable. The arrow indicates the time delay where the phased array arrives at the receiver.

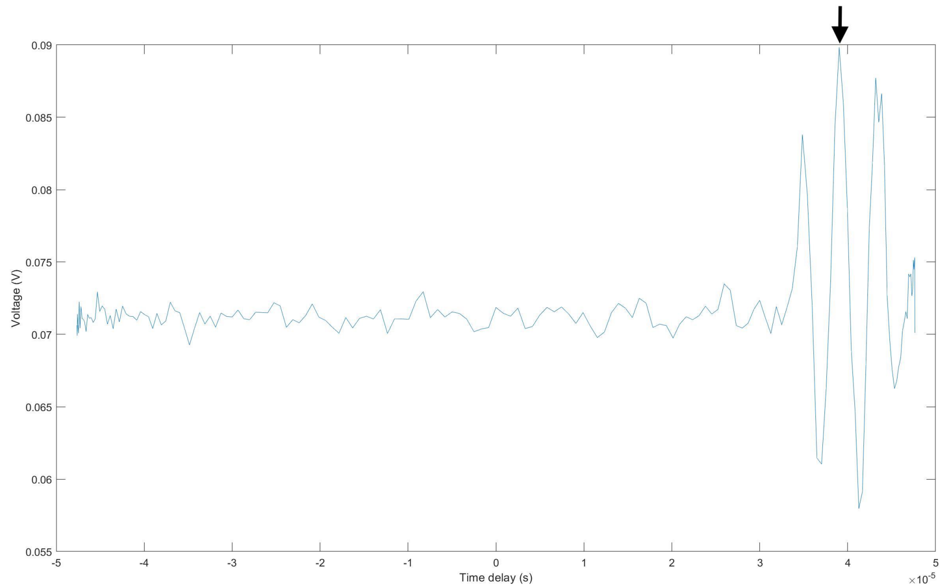

Figure 60: Focus on PWAS8. Signal arriving at receiver PWAS8 for different time delays. Time delay between PWAS1 and PWAS2 is constant, between PWAS1 and PWAS3 is variable. The arrow indicates the time delay where the phased array arrives at the receiver.

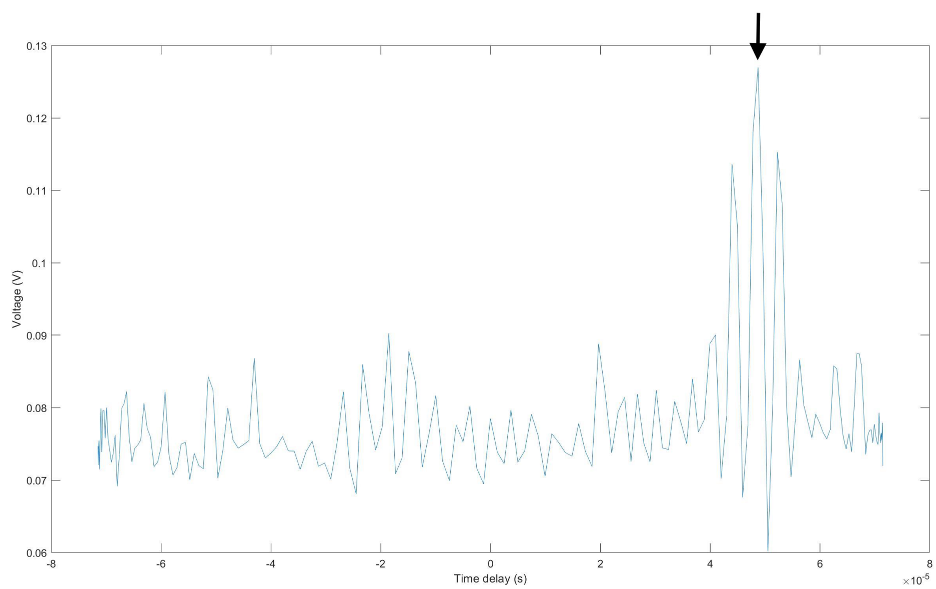

Figure 61: Focus on PWAS8. Signal arriving at receiver PWAS8 for different time delays. Time delay between PWAS1, PWAS2 and PWAS3 is constant, between PWAS1 and PWAS4 is variable. The arrow indicates the time delay where the phased array arrives at the receiver.

A.2.8 Phased array (experimental time delays): TOF found values

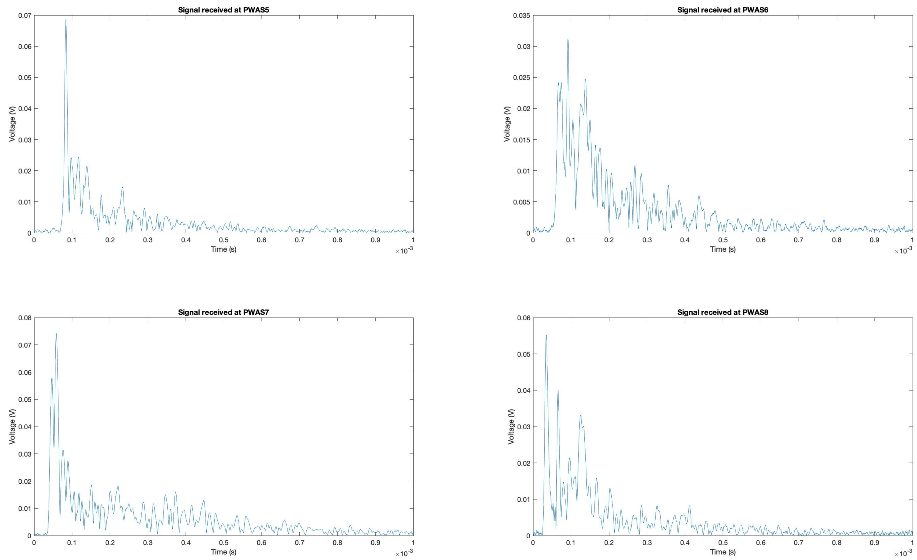

Figure 62: Signal arriving at receivers for TOF found time delays. Focus on PWAS5.

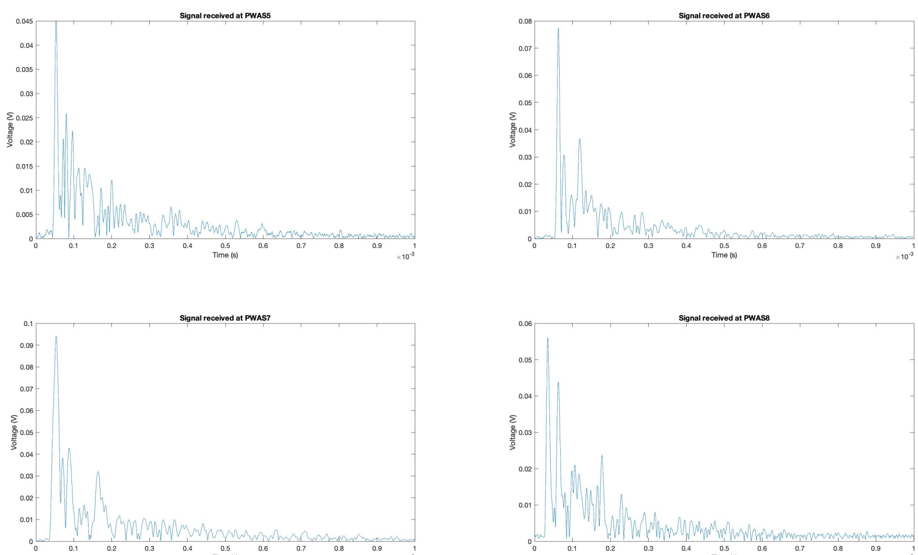

Figure 63: Signal arriving at receivers for TOF found time delays. Focus on PWAS6.

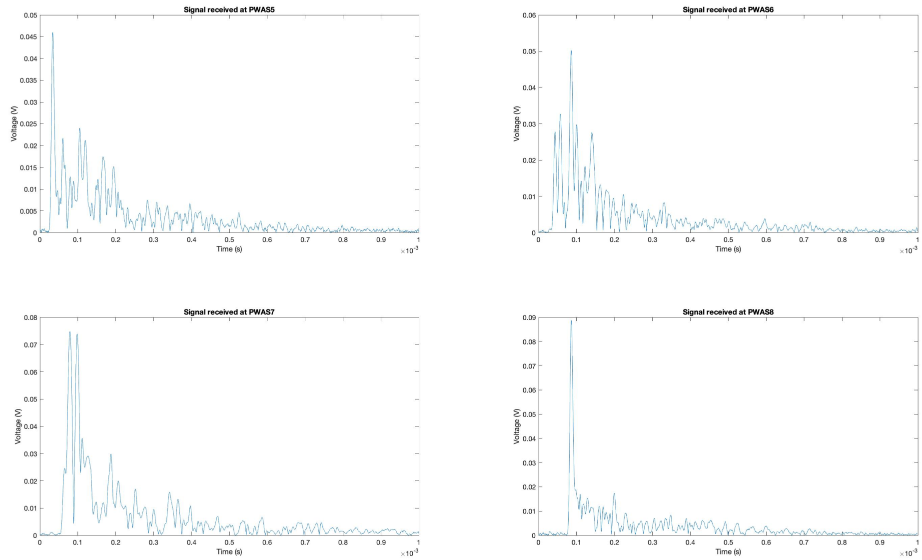

Figure 64: Signal arriving at receivers for TOF found time delays. Focus on PWAS8.